5-15-2013

Lake Kumphawapi — An archive of Holocene paleoenvironmental and paleoclimatic changes in northeast Thailand

Sakonvan Chawchai
Stockholm University, sakonvan.chawchai@geo.su.se

A. Chabangborn
Stockholm University

M. Kylander
Stockholm University

L. Löwemark
National Taiwan University

C.-M. Mörth
Stockholm University

See next page for additional authors

Authors

Sakonvan Chawchai, A. Chabangborn, M. Kylander, L. Löwemark, C.-M. Mörth, M. Blaauw, W. Klubseang, P. J. Reimer, Sherilyn C. Fritz, and B. Wohlfarth

Published in *Quaternary Science Reviews* 68, (May 15, 2013), pp. 59–75; doi: 10.1016/j.quascirev.2013.01.030

Submitted April 14, 2012; revised January 24, 2013; accepted 31 January 31, 2013; published online March 8, 2013.

Lake Kumphawapi — An archive of Holocene paleoenvironmental and paleoclimatic changes in northeast Thailand

S. Chawchai,[1] A. Chabangborn,[1] M. Kylander,[1] L. Löwemark,[2] C.-M. Mörth,[1] M. Blaauw,[3] W. Klubseang,[4, 5] P. J. Reimer,[3] S. C. Fritz,[6] and B. Wohlfarth[1]

1. Department of Geological Sciences, Stockholm University, SE-10961 Stockholm, Sweden
2. Department of Geosciences, National Taiwan University, No 1, Sec. 4, Roosevelt Road, P.O. Box 13-318, 106 Taipei, Taiwan
3. Centre for Climate, the Environment & Chronology (14CHRONO), School of Geography, Archaeology and Palaeoecology, Queen's University Belfast, Belfast BT7 1NN, UK
4. Department of Geology, Faculty of Science, Chulalongkorn University, Bangkok 10330, Thailand
5. Institute for the Promotion of Teaching Science and Technology, 924 Sukhumvit Rd., Bangkok 10110, Thailand
6. Department of Earth and Atmospheric Sciences and School of Biological Sciences, University of Nebraska – Lincoln, 214 Bessey Hall, Lincoln 68588-0340, USA

Corresponding author — S. Chawchai, email sakonvan.chawchai@geo.su.se

Abstract
The long-term climatic and environmental history of Southeast Asia, and of Thailand in particular, is still fragmentary. Here we present a new ^{14}C-dated, multi-proxy sediment record (TOC, C/N, CNS isotopes, Si, Zr, K, Ti, Rb, Ca elemental data, biogenic silica) for Lake Kumphawapi, the second largest natural lake in northeast Thailand. The data set provides a reconstruction of changes in lake status, groundwater fluctuations, and catchment run-off during the Holocene. A comparison of multiple sediment sequences and their proxies suggests that the summer monsoon was stronger between c. 9800 and 7000 cal yr BP. Lake status and water level changes around 7000 cal yr BP signify a shift to lower effective moisture. By c. 6500 cal yr BP parts of the lake had been transformed into a peatland, while areas of shallow water still occupied the deeper part of the basin until c. 5400–5200 cal yr BP. The driest interval in Kumphawapi's history occurred between c. 5200 and 3200 cal yr BP, when peat extended over large parts of the basin. After 3200 cal yr BP, the deepest part of the lake again turned into a wetland, which existed until c. 1600 cal yr BP. The observed lake-level rise after 1600 cal yr BP could have been caused by higher moisture availability, although increased human influence in the catchment cannot be ruled out. The present study highlights the use of multiple sediment sequences and proxies to study large lakes, such as Lake Kumphawapi in order to correctly assess the time transgressive response to past changes in hydroclimate conditions. Our new data set from northeast Thailand adds important paleoclimatic information for a region in Southeast Asia and allows discussing Holocene monsoon variability and ITCZ movement in greater detail.

Keywords: Thailand, Asian monsoon, Lake sediment, Multi-proxy geochemistry, Holocene, Paleoenvironment, Palaeoclimate, ITCZ, Paleomonsoon

1. Introduction

The variation of the Asian monsoon during the Holocene has gained increasing attention during recent decades. It is acknowledged that the strength of the Asian summer monsoon during the Holocene followed insolation patterns, with an increased summer monsoon intensity during the early Holocene, and a gradual decline from the mid-Holocene onwards (Kutzbach, 1981; Wang et al., 2005, 2005a). However the timing of the strengthening and weakening of the monsoon varies significantly among sites as shown by paleorecords across Asia (e.g. An et al., 2000; Morrill et al., 2003; Herzschuh, 2006; Cook et al., 2010; Wang et al., 2010; Yang and Scuderi, 2010; Yang et al., 2011; Cook and Jones, 2012). It is for example still unclear if mid-Holocene changes in monsoon intensity were synchronous or asynchronous between the two major monsoon subsystems, the Indian summer monsoon (ISM) and the East Asian summer monsoon (EASM) (e.g. Dykoski et al., 2005; Chen et al., 2008; Zhao et al., 2009; Cai et al., 2010; Wang et al., 2010; Zhang et al., 2011).

Indochina is located in a key geographic position for studying the interaction between the ISM and the EASM subsystems, but paleoenvironmental data for this large region are still scarce. Paleoclimatic and paleoenvironmental information for Thailand (e.g. Penny, 1998; White et al., 2004; Buckley et al., 2007; Boyd, 2008; Marwick and Gagan, 2011), for example, has only been made available during the last decade.

Nong (Lake) Han Kumphawapi in northeast Thailand (Figure 1A) is one of the largest natural freshwater lakes in the country. Reconstructions of the regional paleoenvironment based on pollen and phytolith studies (Kealhofer and Penny, 1998; Penny, 1998, 1999; White et al., 2004) showed that Kumphawapi's catchment was composed of sparse dryland vegetation and that the basin itself may have been characterized by grassy floodplain and backswamp vegetation between c. 12,400 and 10,400 cal yr BP. Dry climatic conditions were thus inferred for this time interval. The increase in pollen abundance and diversity during the early Holocene (c. 10,400–9000 cal yr BP) suggested a change to more humid climatic conditions (Kealhofer and Penny, 1998), and marked changes in the local flora between c. 9000 and 6800 cal yr BP indicated subsequent high moisture availability. The development of a herbaceous swamp, the increase in charcoal, and the reduction of dryland taxa between c. 6000 and 3000 cal yr BP may have been due to climatic changes or might reflect anthropogenic influences (Kealhofer and Penny, 1998). The re-appearance of secondary forests and the increase in charcoal particles after c. 3000 cal yr BP is interpreted as a result of intensified anthropogenic activities and/or a change in agricultural practices (Kealhofer and Penny, 1998; Penny, 1998). Although several sediment cores had been retrieved and analyzed by Penny (1998), correlations between these proved difficult, especially between sequences from the northern and southern part of the lake.

Further exploration of Lake Kumphawapi's potential as a paleoclimatic and paleoenvironmental archive has shown that the major sedimentary units can be followed across the eastern part of the basin (Wohlfarth et al., 2012). However, the sediment stratigraphies (Penny, 1998; Wohlfarth et al., 2012) also indicate that multiple sub-basins existed in the Kumphawapi basin and that deposition of the major sediment units may have been time-transgressive. The location of the analyzed sediment sequence and the choice of proxies (Penny, 1998; Wohlfarth et al., 2012) can thus generate different temporal and spatial reconstructions of the lake's response to past climatic shifts. The complexity of this large lake system therefore needs to be investigated in more detail before stratigraphic changes in the Kumphawapi basin can be interpreted as an indicator of paleoclimate variability.

Here we present the stratigraphy, a multi-proxy geochemical record, and the chronology for sediment core CP4 (Figure 1B) to reconstruct changes in lake status, groundwater fluctuations and catchment run-off for the past c. 9800 cal yr BP. We then compare our results to those obtained by Penny (1998, 1999) and Wohlfarth et al. (2012) and present a comprehensive paleoclimatic and paleoenvironmental synthesis for the Kumphawapi basin during the Holocene. Moreover, we evaluate Kumphawapi's paleoclimatic record in respect to other Asian monsoon records and place it in wider regional context.

2. Regional setting

Nong Han Kumphawapi (17°11′N, 103°02′E) is located on the Khorat Plateau of northeast Thailand (Figure 1A). The lake is

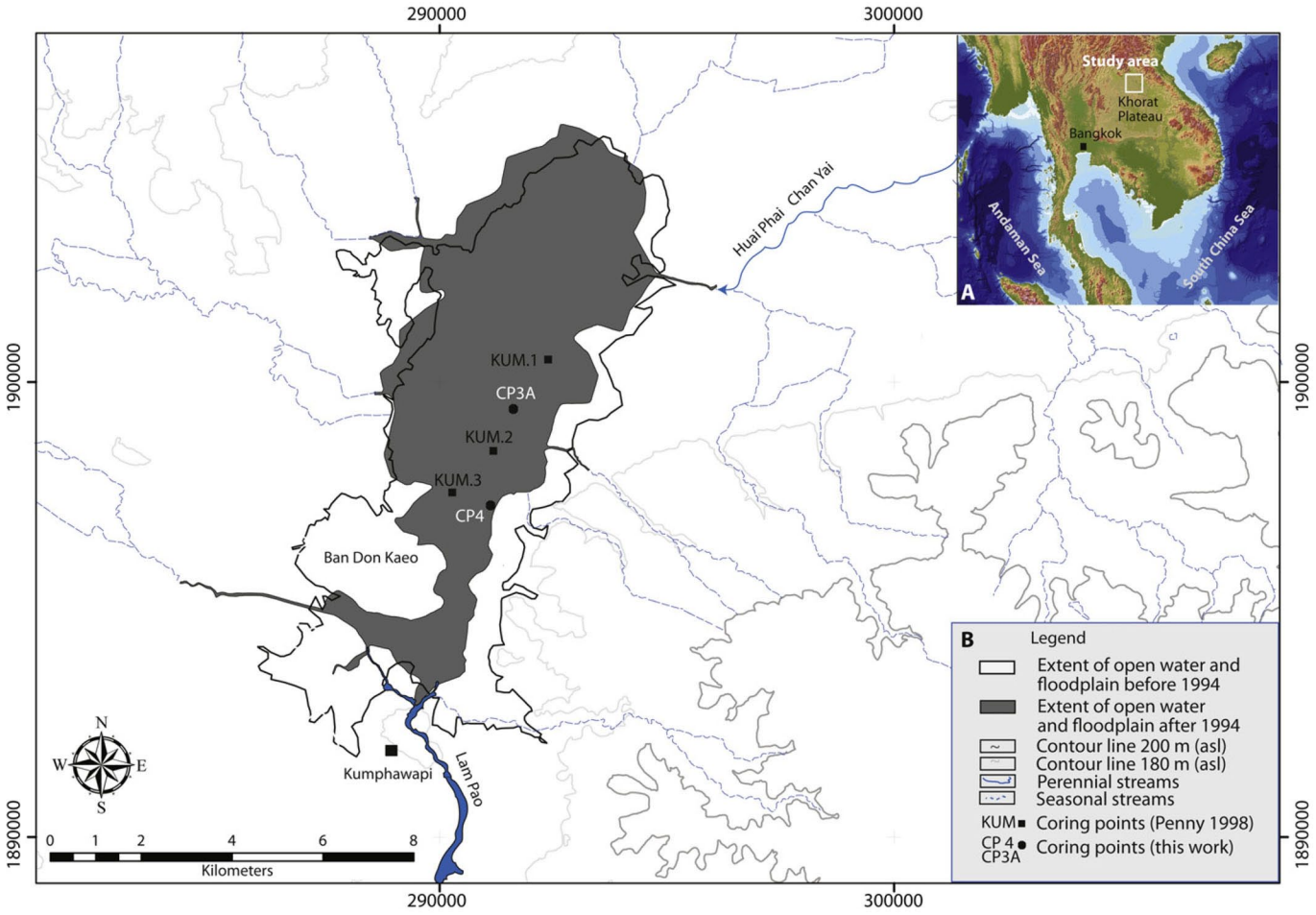

Figure 1. (**A**) Location of the study area on the Khorat Plateau in northeast Thailand. (**B**) Topography around Lake Kumphawapi and the location of coring points. The coordinate system is based on the UTM Grid system (WGS, 1984 zone 48). The extent of open water areas and of the floodplain changed considerably after 1994 due to extensive irrigation work.

situated at approximately 170 m above sea level (asl) and covers an area of about 32 km^2. It occupies a broad alluvial floodplain with low local relief and is surrounded by hills rising to 200 m asl (Figure 1B). Kumphawapi is a shallow lake (<4 m water depth), but it has considerable seasonal fluctuations in water level. The main inflow is through Huai Phai Chan Yai River, which drains the southern slope of the Phu Phan range to the northeast of the lake; other smaller streams enter the lake in the north and west (Figure 1B). The outflow is at the southern end of the lake through the Lam Pao River. Many seasonal streams are active during the summer monsoon season (Figure 1B). Groundwater flow is towards the northwest and geochemically heavily influenced by the evaporites of the underlying Maha Sarakham Formation (Satarugsa et al., 2004).

The lake's extensive floating herbaceous swamp vegetation has been described by Penny (1998, 1999), who noted a domination of grasses (Poaceae including *Phragmites* sp.) and sedges (Cyperaceae), as well as *Eichhornia crassipes*, *Ipomoea aquatica*, *Ludwigia adscendens*, *Ludwigia octovalis*, *Nelumbo nucifera*, *Nymphaea lotus*, *Nymphoides indicum*, *Persicaria attenuata*, *Saccharum* spp., *Typha angustifolia*, and *Salvinia cucullata*. Several fern taxa occur as epiphytic elements on the floating or partially rooted herbaceous substrate.

Present-day climate in the region is tropical monsoonal, with mean air temperatures of around 22–25 °C for November to February, and 27–30 °C for March to October. Mean annual precipitation is about 1455 mm, 88% of which falls during May to October. Monthly mean rainfall (c. 262 mm) occurs during August and September, respectively (Klubseang, 2011). Following the movement of the Intertropical Convergence Zone (ITCZ), humid air masses from the Indian Ocean reach the region between mid-May and mid-October. During August and September tropical cyclones from the east contribute additional precipitation. The northeast monsoon, which dominates between November and February, carries cool and dry air masses from the Siberian anticyclone to the south.

The Khorat Plateau consists of the southern Khorat and the northern Sakon Nakhon basins (Figure 2A), which are filled with Quaternary sediments. These two basins are separated by the northwest-trending Phu Phan anticline, which was formed during the Early Paleocene collision of Southeast Asia and southern China (El Tabakh et al., 2003; Wannakomol, 2005). Kumphawapi is situated in the Sakon Nakhon Basin, c. 36 km southeast of Udon Thani (Figure 2A). The Quaternary sediments on the Khorat Plateau consist mainly of fluvial gravel, sand, silt and clay and have been attributed to high, middle and low terrace deposits. The youngest sediments are valley plain and floodplain deposits (clays, silt and sand and occasional gravelly sand). Quaternary sediments overlie the Neogene Phu Thok Formation (fine- to medium-grained sandstone and siltstone) to the far north of the Kumphawapi Basin. The bedrock to the north and south of the basin is made up of the Cretaceous Maha Sarakham Formation, composed of clastics (clay-stone, siltstone) and three rock salt beds, which are interbedded with gypsum, anhydrite and potash (Figure 2B). The Maha Sarakham Formation overlies the Khok Kruat Formation (sandstone and siltstone), which crops out to the west and east of the Kumphawapi basin (El Tabakh et al., 2003; Wannakomol, 2005; DMR, 2009).

The margins of the Khorat and Sakon Nakhon basins and the upper and lower contacts of the salt units of the Maha Sarakham Formation show strong dissolution (Warren, 1989). Basin subsidence is stronger in the Khorat Basin, resulting in salt domes and leaching of salts to the groundwater, but is less prominent in the Sakon Nakhon Basin (Sattayarak, 1985). Dissolution of salt has led to poor preservation of the upper and middle evaporite beds in the Maha Sarakam Formation and also resulted in the accumulation of anhydrite residues from dissolution of salt in some beds (Figure 2B). Anhydrite-dominated thin residual layers cap the underlying salt beds and follow modern hydrology and topography. The sulfur isotope values of anhydrite samples from the Maha Sarakham salt beds have $\delta^{34}S$ values of +14‰ to +17‰ (CDT), which are very similar to world-wide Cretaceous marine evaporites (El Tabakh et al., 1999). The $\delta^{34}S$ values of the anhydrite nodules, which are present in the upper clastic sedimentary units, are +8.6‰ to +10.9‰ (Figure 2B) and are thus assumed to be the product of continental or mixed-water precipitation (El Tabakh et al., 1999).

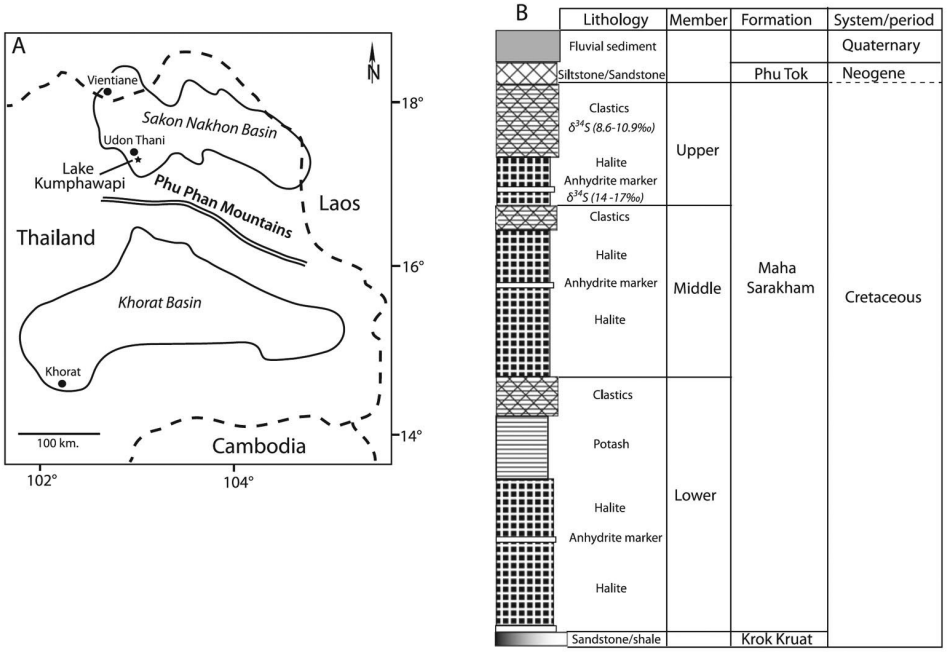

Figure 2. (**A**) Location of the Khorat and Sakon Nakhon basins in northeast Thailand and position of Lake Kumphawapi in the southern Sakon Nakhon basin. (**B**) Simplified lithostratigraphy of the Khorat group (modified from El Tabakh et al., 1999). Note the presence of evaporites in the Maha Sakharam formation.

A seismic and 2-D resistivity survey (Satarugsa et al., 2004) in the surroundings of Lake Kumphawapi showed that the depth of the rock salt layers varies from 50 m to >100 m below the ground surface, and that dissolution of the underlying salt sequences and diapiric salt domes impact the surface morphology of the lake. The peninsula of Ban Don Kaeo constitutes such a salt mound (Figure 1B). It is hypothesized that the formation of the Kumphawapi basin is due to a combination of rock salt cavity collapse and gradual land subsidence (Satarugsa et al., 2004).

3. Materials and methods

The sediment sequence of CP4 was obtained in January 2010 from the southern part of Nong Han Kumphawapi (Figure 1B) using a modified Russian corer (7.5 cm diameter, 1 m length) and 50 cm overlap between the 1-m core segments. The sediment cores were wrapped in plastic and placed in PVC tubes for transport to the Department of Geological Sciences at Stockholm University, Sweden. The cores were stored in a cold room (at 4 °C) until analyses. Laboratory work included detailed lithostratigraphic descriptions; non-destructive XRF scanning measurements (specifically Si, Zr, K, Ti, Rb, and Ca); geochemistry (carbon, nitrogen, and sulfur elemental and isotopic composition; biogenic silica analyses) and ^{14}C dating.

The core surfaces were carefully cleaned, and each 1-m long core segment was scanned with the Itrax XRF core scanner at 5 mm resolution using a Mo tube set at 30 kV and 30 mA for 60 s/point. Information about incoherent (Compton) and coherent (Rayleigh) scattering is acquired during the measuring process. The incoherent/coherent scattering ratio (inc/coh) increases with higher organic carbon concentrations and can be used as a qualitative indicator of the organic matter content (Corella et al., 2010). The elemental data were averaged over 1 cm intervals and smoothed using a 3 point running mean (peak area). The curve was then divided by incoherent and coherent scattering to obtain normalized peak areas. These account for changes in organic content, water content, and sediment density during analysis (Kylander et al., 2011).

The lithostratigraphy of each core segment was described in the laboratory. Correlations between the overlapping 1-m cores segments were done visually, based on stratigraphic markers, but were aided by major XRF curve features. The sedimentary sequence between 7.03 and 2.00 m depth was subdivided into 23 layers, which were grouped into six lithostratigraphic units (Table 1).

Contiguous 1-cm intervals were sub-sampled for loss-on-ignition (LOI) analysis to obtain an estimate of the organic matter content of the sediments. The samples were dried at 105 °C, homogenized, and combusted at 550 °C. Sub-samples for total organic carbon (TOC), total nitrogen (TN), and stable isotopes ($\delta^{13}C_{org}$, $\delta^{15}N$ and $\delta^{34}S$) were taken at 30-cm intervals in the lower part of the sediment sequence, where the LOI curve suggests less variability, and at 1-cm intervals in the upper part, corresponding to 110 samples. The samples were freeze-dried and homogenized before analysis without prior removal of carbonate carbon, because the inorganic carbon content of the sediments is low. %TOC, %TN, $\delta^{13}C_{org}$, $\delta^{15}N$ and $\delta^{34}S$ were measured on a Carlo Erba NC2500 elemental analyzer, which is coupled to a Finnigan MAT Delta + mass spectrometer. $\delta^{13}C_{org}$, $\delta^{15}N$ and $\delta^{34}S$ values are reported in ‰ relative to Vienna PeeDee Belemnite (VPDB, for C), to AIR (for N), and to Canyon Diablo Troilite (CDT, for S) standards, respectively. The analytical error was ±0.15‰ for $\delta^{13}C$ and $\delta^{15}N$, and ±0.2‰ for $\delta^{34}S$.

Carbon: nitrogen (C/N) atomic ratios were calculated according to Meyers and Teranes (2001) and are used here to estimate changes in aquatic and terrestrial organic matter sources. Since interpretations of sedimentary $\delta^{15}N$ are rather difficult (Meyers, 1997; Brenner et al., 1999; Meyers and Teranes, 2001). Therefore, C/N values, $\delta^{13}C$ and $\delta^{15}N$ isotope values need to be interpreted together. Here we employ $\delta^{34}S$ to assess changes in the groundwater table using a two source isotopic mixing model (Fry, 2006). We hypothesize that a lowering of the groundwater level would result in a change in the $\delta^{34}S$ signature, because anhydrite samples from the different sedimentary units of the Maha Sarakham formation display distinct changes in $\delta^{34}S$ values (El Tabakh et al., 1999).

Samples for biogenic silica (BSi), which is a measure of amorphous silica in the sediment and a good proxy for the abundance of diatoms and other siliceous microfossils (sponges, phytoliths) (Conley, 1998), were taken at the same levels as those for TOC, TN and CNS isotope analyses. The freeze-dried sediment samples were analyzed after pre-cleaning with H_2O_2 and HCl to remove organic matter and carbonate as suggested by Mortlock and Froelich (1989) and Saccone et al. (2006). The BSi content of the sediments was determined by alkaline extraction of 30 mg of sediment in 40 mL of 1% Na_2CO_3 solution, over a 5 h period with sub-samples taken at 3 (within), 4 and 5 h and neutralized with 0.21 N HCl as described by Conley and Schelske (2001). The extracts were analyzed for dissolved silica (DSi) by ICP-OES (Varian Vista Ax), and the concentration data were plotted against depth/time. The sub-sample *y*-intercept

Table 1. Lithostratigraphic description of sediment sequence CP4. See Figure 1B for the location of core CP4. sLB = sharp lower boundary, gLB = gradual lower boundary, vgLB = very gradual lower boundary.

Depth (m) below water surface	Lithostratigraphic description	Layer	Units
2.00–2.15	Dark brown fine detritus algae gyttja, gLB	1	3b
2.15–2.37	Dark grey to brown clayey algae gyttja with coarse organic material, gLB	2	3a
2.37–2.43	Dark grey to brown clayey gyttja, gLB	3	
2.43–2.49	Dark brown to dark grey clayey gyttja with lenses of coarse organic material; transition zone between layers 3 and 5, gLB	4	
2.49–2.63	Black to dark brown coarse detritus clayey gyttja, gLB	5	
2.63–2.68	Dark brown to black, clayey gyttja with visible organic material, gLB	6	
2.68–2.78	Dark brown to black gyttja with less clay and more organic material than layer 6, very compact, gLB	7	
2.78–2.94	Brown (when fresh), dark brown to black (when oxidized) peat with reddish-brown wood/organic fragments, softer than layer 7, many seeds, not humified, gLB	8	2b
2.94–3.03	Dark brown coarse detritus gyttja/peat, slightly compact, gLB	9	
3.03–3.26	Dark brown coarse detritus gyttja/peat, less compact than layer 9, gLB	10	
3.26–3.28	Brown clayey algae gyttja, sLB	11	2a
3.28–3.39	Dark grey clayey gyttja; oxidizes rapidly, visible plant remains, sLB	12	
3.39–3.55	Brownish-grey gyttja clay, gLB	13	
3.55–3.77	Dark grey gyttja clay, some visible plant remains, gLB	14	
3.77–3.80	Transition zone between layers 14 and 16 boundary	15	
3.80–4.55	Greenish-grey gyttja clay	16	1b
4.55–5.40	Greenish-grey gyttja clay, gLB	17	
5.40–5.93	Greenish-grey silty gyttja clay, compact; fine sand layer between 5.69 and 5.72 m	18	1a
5.93–6.05	Transition zone between layers 20 and 18	19	
6.05–6.41	Light brown silty gyttja clay/clayey silt, fine sand layer between 6.22 and 6.26, gLB	20	
6.41–6.58	Light brown silty gyttja clay/clayey silt; FeS layer at 6.46–6.47	21	
6.58–6.76	Light brown clayey gyttja silt	22	
6.76–7.03	Dark grey silty gyttja clay	23	

was considered to be the BSi (wt %) content corrected for a simultaneous dissolution of silica from minerals.

Sixteen samples were selected for ^{14}C dating (Table 2). The samples were sieved (mesh size 0.5 cm) under running tap water, and sieve remains were stored in deionized water. Sieve remains were identified under a stereomicroscope and carefully cleaned in deionized water. Charcoal, seeds, leaves, insects, twigs and small wood fragments were chosen for dating. The selected samples were dried overnight at 105 °C in pre-cleaned glass vials and were then submitted to the ^{14}CHRONO Centre at Queen's University, Belfast for analysis. Pre-treatment of the charcoal and wood samples followed the acid-base-acid method (de Vries and Barendsen, 1952). The samples were rinsed in deionized water and dried at 50 °C overnight, then weighed into pre-combusted quartz tubes with silver and CuO and combusted at 850 °C overnight to produce CO_2. Samples with less than 0.8 mg of carbon were graphitized in the presence of hydrogen on an iron catalyst at 560 °C for a maximum of 4 h according to the Bosch-Manning Hydrogen Reduction Method (Vogel et al., 1984). The CO_2 from the larger samples was converted to graphite on an iron catalyst using the zinc reduction method (Slota et al., 1987). The $^{14}C/^{12}C$ ratio and $^{13}C/^{12}C$ were measured on a 0.5 MV National Electrostatics Corporation accelerator mass spectrometer (AMS). The radiocarbon age and one standard deviation were calculated following the conventions of Stuiver and Polach (1977) using the Libby half-life of 5568 years and a fractionation correction based on $\delta^{13}C$ measured on the AMS which accounts for both natural and machine fractionation. The sixteen ^{14}C dates were calibrated with the Calib 6.0 online program using the northern hemisphere terrestrial calibration curve (Reimer et al., 2009) (Table 2).

4. Results

4.1. Lithostratigraphy and geochemistry of CP4

The gyttja silts and gyttja clays (7.03–5.40 m depth) of unit 1a have low, but variable LOI (3–6%), TOC (0.5–1.6%) and BSi (0.8–1.8%) values, and $\delta^{15}N$ values are of ~+3‰ (Figure 3 and Figure 4A, B, Table 1). The C/N ratio is around 18 in the lowermost part, declines to 11–13 in the middle part and increases to 20–21 in the upper part of unit 1a. $\delta^{13}C$ values decrease gradually from −18 to −24‰. Sulfur isotopes were not measured because of the low organic carbon content. The XRF normalized and peak area curves display similar patterns, although each element has different absolute counts (Figure 5A). Si and Zr co-vary, and K, Ti and Rb correlate well. The XRF data suggests a sub-division into two sub-units: layers 23–20 show higher values of K, Ti and Rb as compared to Si and Zr, while the opposite is the case for layer 18. The Zr/Rb ratio shows considerable variability with depth and becomes significantly higher in layer 18. These observations are corroborated by statistical correlation matrices, which confirm two groups of elements, Si and Zr; and K, Ti and Rb (Figure 5B).

In the grey gyttja clay of unit 1b (5.40–3.80 m depth) LOI (4–6%) and TOC (1–1.5%) values remain low and the C/N ratio is around 13–16 (Figure 3). BSi values fluctuate between 1.0 and 1.4% and show two peaks of 2.69% and 2.72%. $\delta^{13}C$ values are −23 to −24‰, $\delta^{15}N$ values decrease from +3.5 to +1.5‰ and $\delta^{34}S$ values are +8.6 to +11.8‰ (Figure 3 and Figure 4A–C). Elemental curves for Si, K, Ti, Rb and Ca show similar variations and have values comparable to layers 23–20 in unit 1a (Figure 5A). Si, K, Ti and Ca are significantly lower between 4.7 and 4.6 m depth, and the Zr/Rb ratio is slightly higher between 4.7 and 4.2 m. The major elements in unit 1b show clear affinities between K, Ca, and Rb on one side, and Si and Ti on the other side (Figure 5B). This is different from unit 1a, where Si correlates with Zr.

The sediments of unit 2a change from gyttja clay in layers 15–13 (3.80–3.39 m depth) to clayey gyttja in layer 12 (3.39–3.28 m depth), and to algae gyttja in layer 11 (3.28–3.26 m depth) (Table 1). This change is reflected by a gradual increase in LOI and TOC values to 10% and 5%, respectively (Figure 3). The C/N ratio varies around 14–18, BSi values decrease markedly at 3.69 m depth and remain low throughout and $\delta^{13}C$ values of around −22 to −24‰ are similar to those in unit 1b (Figs. 3, 4A). $\delta^{15}N$ values in the lower part of unit 2a are close to those of unit 1b, but <0‰ in the upper part. $\delta^{34}S$ values fluctuate slightly, but range between +12.2 and +13‰, which is higher than in unit 1b (Figure 4B, C). All elemental values are lower than those in units 1a and 1b. The correlation matrix suggests a strong correlation between the elements of Si, K, Ti and Rb (Figure 5B). The Zr/Rb ratio indicates that sediments in layer 12 (3.39–3.28 m depth) are finer grained than those in layers 15–13 (3.80–3.39 m depth) (Figure 5A).

The change to peaty gyttja (layers 10–9, 3.26–2.94 m depth) and peat (layers 8, 2.94–2.78 m depth) in unit 2b (Table 1) is reflected by high LOI and TOC percentages. LOI attains values of between 22 and 74% and TOC increases from 11 to 40% (Figure 3). It is noteworthy that both %LOI and %TOC decrease markedly in the peat between 2.91 and 2.93 m depth. BSi values fluctuate between 0.2 and 0.8%, which is relatively low, as compared to unit 1a and b. C/N ratios increase from 16 to 27, $\delta^{13}C$ values decrease from −25 to −27‰, and $\delta^{15}N$ values fluctuate between +0.1 and +0.9‰ (Figs. 3 and 4D, E). $\delta^{34}S$ values

Table 2. ^{14}C dates for Lake Kumphawapi. Core depth (in m) is given below the water surface. Calibration of the ^{14}C dates was made with the Calib 6.0 online program (http://calib.qub.ac.uk/calib/calib.html) and is according to Reimer et al. (2009). The sedimentary units relate to those shown in Figure 3 and Table 1.

Lab ID	Core depth (m)	^{14}C date BP ±1 sigma	Dated material	Calibrated age (2 sigma) range (cal yr BP)	Sedimentary unit
UB-16743	2.50–2.54	547 ± 23	Seeds, leaf fragment, charcoal	520–631	3a
UB-16744	2.59–2.61	1306 ± 24	Seeds, leaf fragment, insects	1179–1291	3a
UB-18070	2.63–2.65	1493 ± 23	Charcoal, seeds	1319–1411	3a
UB-16745	2.94–2.96	5731 ± 28	Seeds, leaf fragments, insects, charcoal	6446–6632	2b
UB-18071	3.09–3.11	6015 ± 31	Leaf fragments, seeds	6781–6954	2b
UB-18073	3.83–3.86	6726 ± 56	Leaf fragments, seeds	7496–7675	2a
UB-16746	4.69–4.71	7902 ± 34	Large seed	8598–8792	1b
UB-16747	5.25–5.27	8328 ± 38	Mix of plant material	9254–9466	1b
UB-16748	5.45–5.47	8711 ± 33	Leaf fragments, seeds	9549–9776	1a
UB-16749	5.45–5.47	8702 ± 34	Wood fragment	9549–9746	1a
UB-16750	5.53–5.55	8631 ± 40	Leaf fragments	9534–9680	1a
UB-16751	5.67–5.69	8698 ± 44	Leaf fragments, seeds, wood	9544–9784	1a
UB-16752	5.83–5.85	8723 ± 36	Leaf fragments, seeds	9552–9798	1a
UB-16753	5.95–5.97	8734 ± 33	Leaf fragments, seeds	9559–9823	1a
UB-16754	5.95–5.97	8797 ± 33	Wood fragments	9678–9934	1a
UB-16755	6.05–6.07	8729 ± 40	Small twigs	9556–9832	1a

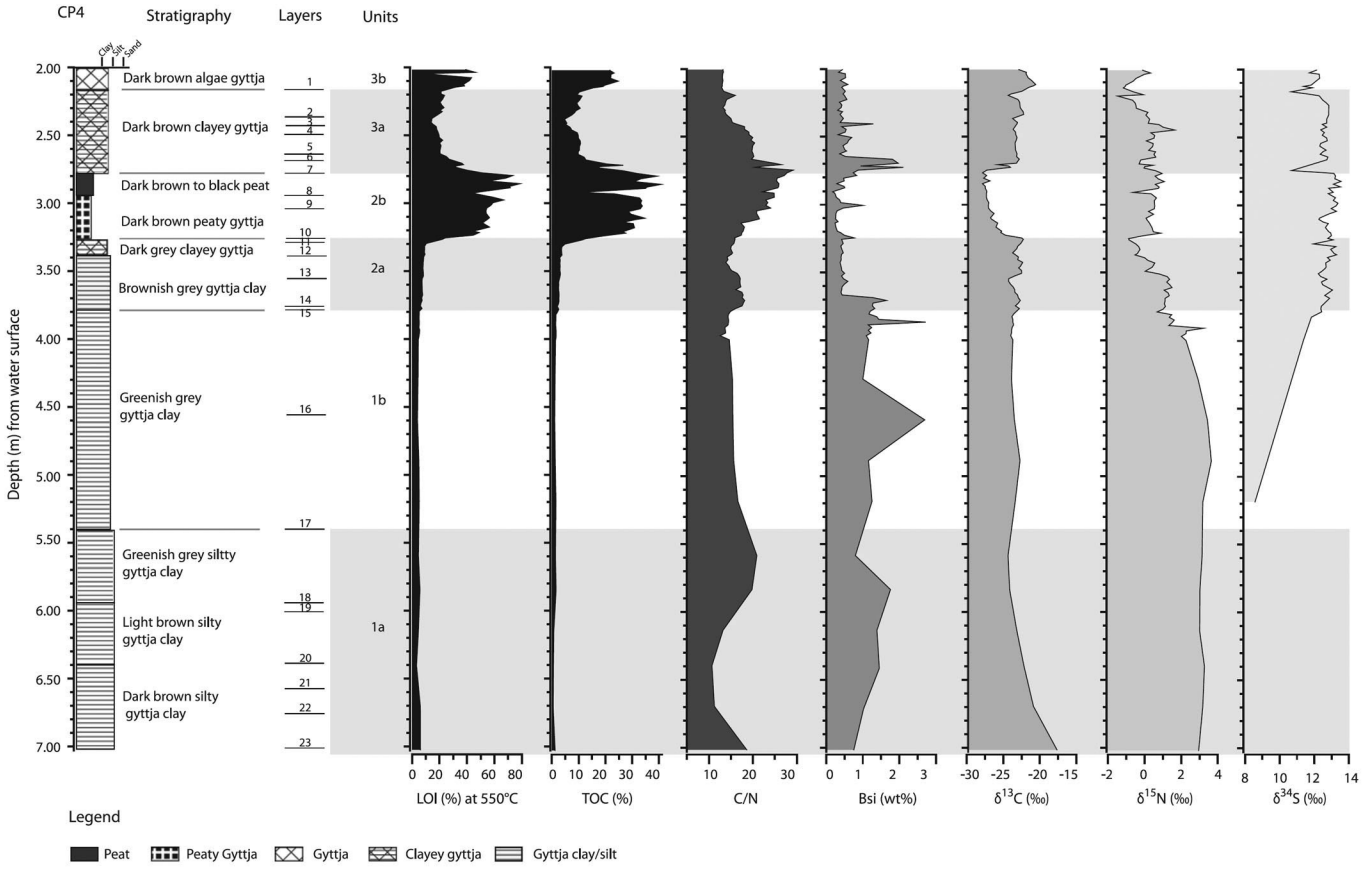

Figure 3. Lithostratigraphy and geochemistry of sediment sequence CP4. See Figure 1B for the location of the sediment core.

fluctuate between +12.2 and +13.2‰ in the peaty gyttja but reach +12.8 to +13.5‰ in the peat layer (Figure 4F). Major elements have much lower values than in unit 1a and b but show a clear correlation between Si, Zr, K, Ti and Rb (Figure 6B). The marked peak in Si, Zr and Ti at 2.91–2.93 m depth in the peat layer coincides with the decrease in %LOI and %TOC and suggests incorporation of silicate minerals. Also, the comparably high Zr/Rb ratio between 2.92 and 2.88 m depth indicates the presence of mineral material (Figure 6A). At 2.84 m depth values of K, Ti and Rb are again comparably high, at the same time as %LOI and %TOC are low. These higher values for K, Ti and Rb suggest the presence of clay particles.

In the clayey gyttja of unit 3a %LOI decreases from 50 to 14% and %TOC from 32 to 5% in layers 7–3 (2.78–2.37 m depth). The C/N ratio declines from 29 to 15, BSi values are variable (0.5–2.1%) and $\delta^{13}C$ values range from −28 to −23‰ (Figure 3; 4G). In layer 2 (2.37–2.15 m) %LOI increases to 24% and %TOC to 10%. BSi values remain low (<0.5%), the C/N ratio is around 13–16, and $\delta^{13}C_{org}$ has values of around −22 to −24‰. $\delta^{34}S$ values vary from +11 to +13‰ throughout unit 3a (Figure 4I). Elemental values gradually increase between 2.78 and 2.37 m and subsequently decline (Figure 7A). The increase and subsequent decline corresponds well to the decrease and increase in %LOI and %TOC. All elements display similar patterns, except for Ca, and good correlations ($r > 0.7$) exist between Si, Zr, K, Ti, Rb and Ca (Figure 7B).

The algae gyttja layers of unit 3b (2.15–2.00 m) are characterized by LOI and TOC values of up to 46% and 25%, respectively. The high LOI and TOC values, and stable BSi percentages (<0.5%) are similar to those in unit 2b, but C/N ratios of 13 and $\delta^{13}C_{org}$ values of around −21‰ are very different from those in unit 2b (Figure 3). $\delta^{15}N$ values are below 0, and $\delta^{34}S$ values range between +11 and +12‰ (Figure 4H, I). All major elements display similar patterns and have low values (Figure 7A), comparable to those in the upper part of unit 3a and in unit 2b, except for Ca. Calcium has higher values in units 3a and b. The Zr/Rb ratio is fluctuating, and a correlation exists between Si and Ti, and between K, Ti, Rb and Ca (Figure 7B).

4.2. Chronology

The 16 AMS ^{14}C dates do not show any age-reversals (Table 2 and Figure 8). However the dates in unit 1a are all of comparable ages, indicating a rapid sediment accumulation. Moreover, the dates suggest a long-lasting hiatus between 2.94 and 2.65 m depth. This gap could not be narrowed by more ^{14}C dates, since the sieve remains contained only larger wood fragments, which were not selected for dating because they might have been reworked (Wohlfarth et al., 2012). An age-model was constructed using Bacon, a Bayesian statistics-based routine that models accumulation rates by dividing a sequence into many thin segments and estimating the (linear) accumulation rate for each segment based on the (calibrated) ^{14}C dates (Reimer et al., 2009) together with prior information (Blaauw and Christen, 2011). The prior information includes assumptions about the accumulation rate (a gamma distribution with a mean of 20 yr/cm and shape 1.1), the memory or variability of the accumulation rate between neighboring segments (a beta distribution between 0 and 1, mean 0.7, strength 4), and hiatus length (a gamma distribution with mean 3000 and shape 1, set at 2.925 m depth as the most likely depth for the hiatus given geochemical information). Since the Bacon model considers very high sediment accumulation rates unlikely, the model does not follow through the 'vertical' group of ^{14}C dates in unit

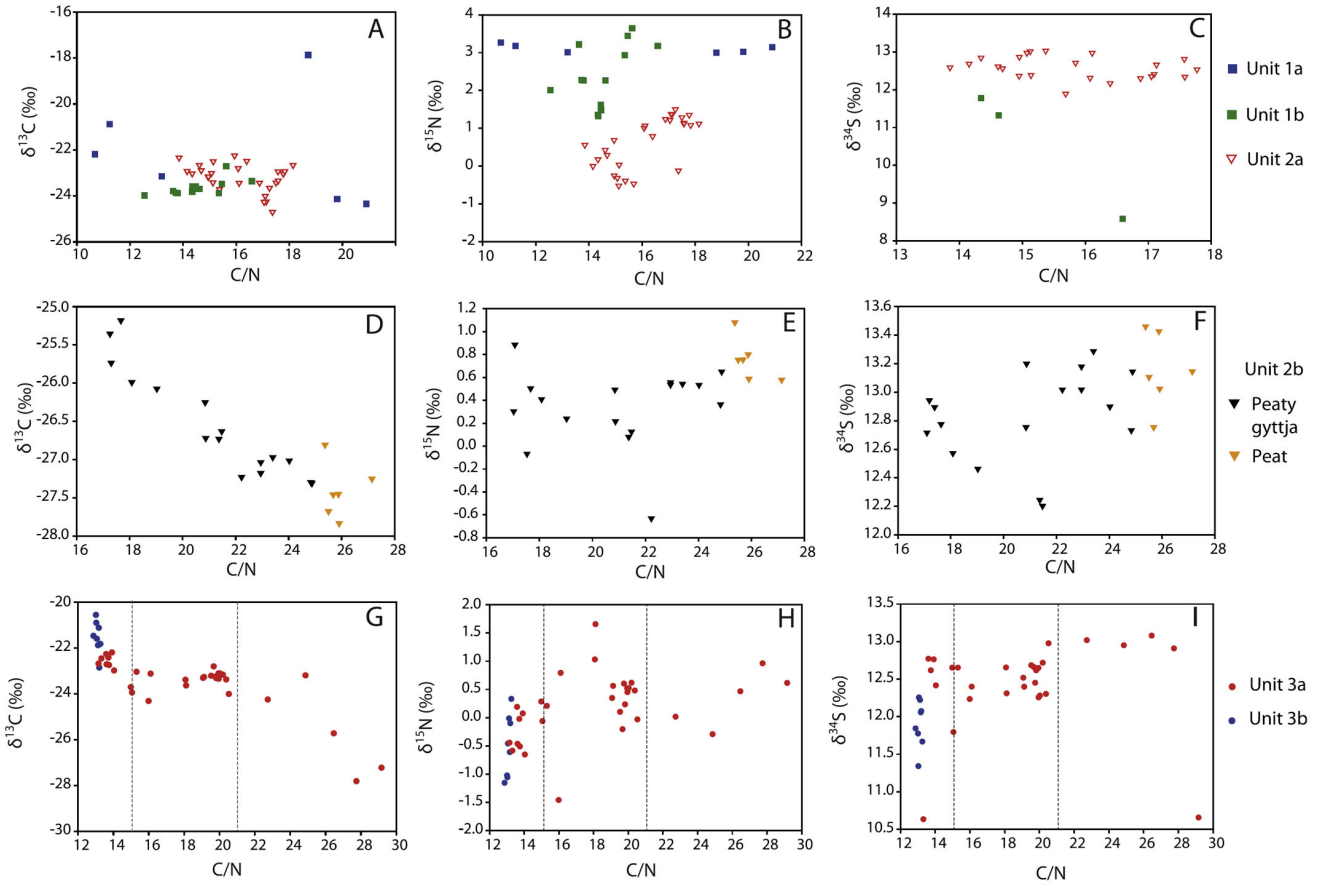

Figure 4. A–I geochemistry bi-plot of CNS isotopes vs C/N, divided into the different stratigraphic units. See Figure 3 for the stratigraphy of units 1a–3b.

1a. Instead, since the ^{14}C dates within that section provide little guidance, the Bacon model mostly followed here the prior information on sediment accumulation rates.

Reconstructed sedimentation rates were high in unit 1a, which is dated to between >9800 and c. 9600 cal yr BP. Lower sedimentation rates are assumed during the deposition of units 1b and 2a, which date to c. 9600–7600 cal yr BP, and 7600-7000 cal yr BP, respectively (Figure 8). The lower part of unit 2b (layers 11–9) has an age of between c. 7000 and approximately 6500 cal yr BP, although we cannot exclude that parts of unit 2b have been affected by the overlying hiatus. As such the younger age of 6500 cal yr BP constitutes a minimum estimate. However the duration of the overlying peat (layer 8) cannot be estimated, since its lower boundary coincides with a long-lasting hiatus. Major element counts in the peat give evidence for the presence of mineral material, which could indicate a break in peat growth and as such the occurrence of a hiatus. The upper units 3a and b are dated to between AD 1600 and present day.

5. Interpretation of the lithostratigraphy and geochemistry of CP4

5.1. Unit 1a: >9800–c. 9600 cal yr BP

The low organic matter and carbon content of these rapidly accumulated sediments suggest low lake organic productivity or that most of the organic material had become decomposed and oxidized. The C/N ratio and the $\delta^{13}C$ values show that the sediments contain a mix of aquatic and terrestrial organic material (cf. Meyers, 1997; Meyers and Teranes, 2001), but that the terrestrial component increases around 9700 cal yr BP. The association of K, Ti and Rb in the lower part of unit 1a is typical for fine-grained sediments, such as clay and could indicate weathering of clay minerals in the catchment. Zr and Si on the other hand are often associated with silty sediments and coarse-grained minerals, and the high Zr/Rb ratio in the upper part of unit 1a can therefore be taken as a proxy for coarser grain size (Dypvik and Harris, 2001). The change in grain size between the lower and upper sub-unit, suggests that transport mechanisms to the lake had changed. This change could have been caused by higher run-off and higher precipitation, which would have brought coarser mineral material and terrestrial organic matter from the surroundings into the lake. Sediment composition and geochemical parameters in unit 1a thus might indicate a change from a lake with predominantly aquatic organic material and less run-off to a lake with more terrestrial input and possibly also higher run-off.

5.2. Unit 1b: c. 9600–c. 7600 cal yr BP

Lake organic productivity remains low and most of the organic material in the sediments is derived from a mix of terrestrial and aquatic organic matter sources as indicated by $\delta^{13}C$ and C/N ratio (cf. Meyers, 1997; Meyers and Teranes, 2001). $\delta^{34}S$ values of +8 to +12‰ are in the range of the isotopic composition of the non-marine sulfur anhydrite nodules (Figs. 2B and 3), which are part of the uppermost clastic unit of the Maha Sarakham Formation underlying the lake basin (El Tabakh et al., 1999). The sulfur isotope values suggest that the groundwater that affected the sulfur system in the lake was influenced by the dissolution of anhydrite nodules in the upper-

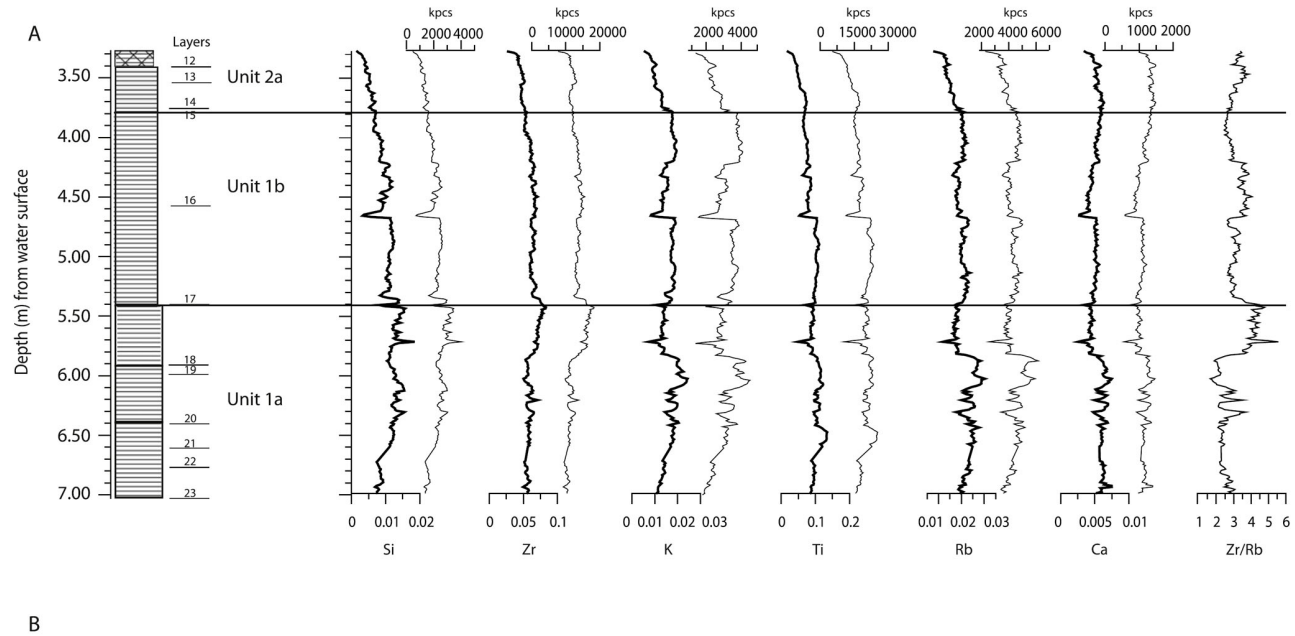

B

Unit 1a

	Zr	K	Ti	Rb	Ca
Si	0.72	0.29	0.25	-0.08	-0.41
Zr		-0.18	-0.10	-0.46	-0.69
K			0.79	0.88	0.62
Ti				0.72	0.45
Rb					0.75

Unit 1b

	Zr	K	Ti	Rb	Ca
Si	0.38	0.18	0.80	-0.09	-0.04
Zr		-0.54	0.06	-0.56	-0.67
K			0.31	0.79	0.87
Ti				0.21	0.06
Rb					0.67

Unit 2a

	Zr	K	Ti	Rb	Ca
Si	0.27	0.78	0.85	0.64	0.56
Zr		0.02	-0.03	0.12	0.03
K			0.80	0.88	0.42
Ti				0.70	0.59
Rb					0.27

Figure 5. (**A**) Lithostratigraphy and selected geochemical variables for units 1a, 1b and 2a. The thicker left curve for each element represents the normalized peaks (see text for explanation) and the thinner right curves for each element the peak area in counts/second/measuring point (kpcs). The Zr/Rb curve is a proxy for grain size variations. See Table 1 and Figure 3 for the stratigraphic legend. (**B**) Correlation matrices (*r* values) for selected elements in units 1a, 1b and 2b.

most clastic unit of the Maha Sarakham Formation (Figure 2B). The major elements (Si, K, Ti, Rb and Ca) have an association with fine-grained mineral particles, which would imply transport of clay and silt-sized particles to the lake. In contrast to unit 1a, Si correlates here with Ti, which together with peaks in BSi values, could indicate a biogenic source for Si. The sediment geochemical parameters thus suggest the presence of a lake with more stable conditions than before, although lake organic productivity remained low.

5.3. Unit 2a: c. 7600–c. 7000 cal yr BP

The sediments and the different proxies indicate a gradual decrease in grain size and an increase in lake organic productivity, which suggests minor run-off and stable lake conditions. The organic material was composed of a mix of terrestrial and aquatic sources (cf. Meyers, 1997; Meyers and Teranes, 2001). The shift observed in the $\delta^{15}N$ values could indicate a change in catchment vegetation and might compare to the change in vegetation from predominantly Bambusoid grasses to *Cyperaceae* and *Oryza* species, sedges and ferns observed in KUM.3 (Figure 1B) (Kealhofer and Penny, 1998; Penny, 1998, 1999).

5.4. Unit 2b: c. 7000 – c. 6500 cal yr BP

The high organic matter and organic carbon values, together with the C/N ratio and the $\delta^{13}C$ values show that greater amounts of terrestrial plants were preserved in the sediment (cf. Meyers, 1997; Meyers and Teranes, 2001). The peaty gyttja and the overlying non-humified peat, together with the geochemical proxies, suggest that the shallow lake had transformed into a wetland and subsequently into a peatland (Figure 3, Table 1). This shift would imply a lowering of the groundwater level and/or reduced precipitation and as such drier climatic conditions. The increase in $\delta^{34}S$ values in the peat would suggest that the groundwater level had reached the lower units of the Maha Sarakham formation (El Tabakh et al., 1999) (Figure 2B).

The distinct decline in organic carbon content and the concomitant increase in Si, Zr and Ti at 2.93–2.91 m depth, a higher Zr/Rb ratio at 2.92–2.88 m depth and lower organic carbon content and higher K, Ti and Rb counts at 2.84 m depth suggest intervals with increased contribution of mineral material. These could have been transported to the lake by surface run-off due to wetter conditions. However, the $\delta^{34}S$ values give no indication of a marked shift in the groundwater level, which should respond to a change in hydroclimate. Another explanation for the presence of mineral particles in the peat could be wind transport during dry conditions. Since physical weathering is elevated during dry periods, stronger winds could have transported sediment material to the lake. If this assumption holds true, the intervals characterized by higher contributions of mineral particles could signify marked dry periods.

5.5. Unit 3a and b: c. 1600 cal yr BP to present

The clayey gyttja sediments and the geochemical proxies indicate the re-establishment of a shallow lake around 1600 cal yr BP. The C/N ratio, $\delta^{13}C$ and $\delta^{15}N$ values suggest that the lake organic material was composed of a mix of terrestrial and aquatic organic matter sources (cf. Meyers, 1997; Meyers and Teranes, 2001), and the sulfur isotope values imply a rise in the groundwater table. Higher values for the elemental data suggest higher contributions of mineral material and higher

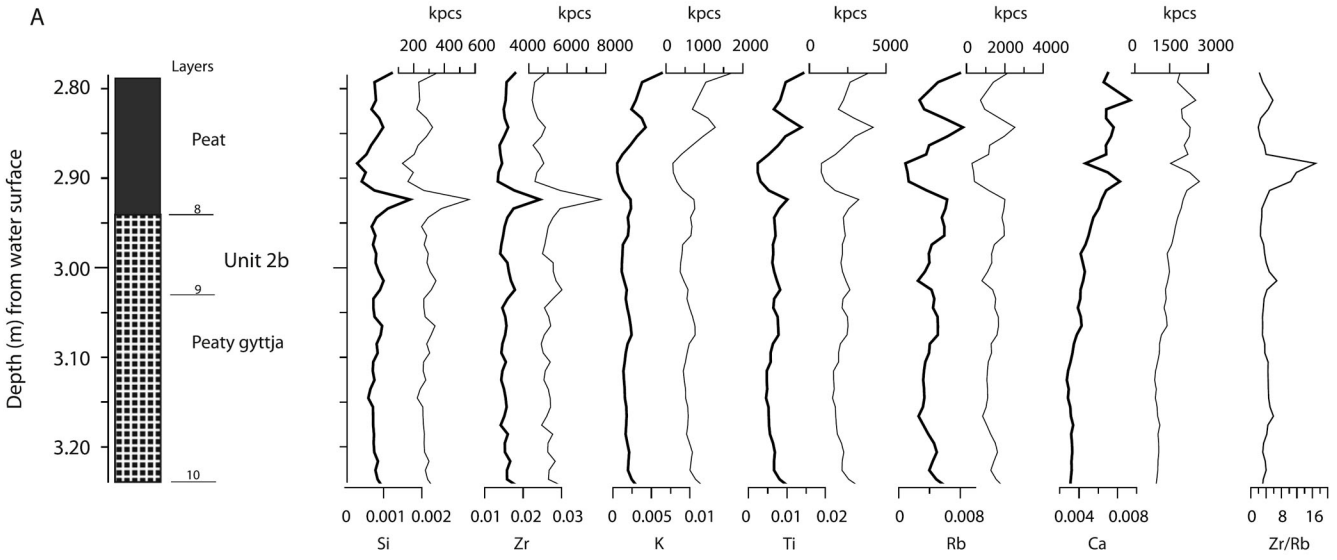

B

Peat (2.78-2.94 m depth)

	Zr	K	Ti	Rb	Ca
Si	0.84	0.47	0.69	0.75	-0.09
Zr		0.01	0.28	0.41	-0.18
K			0.92	0.81	-0.14
Ti				0.94	-0.08
Rb					-0.12

Peaty gyttja (2.94-3.29 m depth)

	Zr	K	Ti	Rb	Ca
Si	0.93	0.86	0.94	0.71	-0.14
Zr		0.89	0.89	0.73	-0.22
K			0.95	0.85	0.08
Ti				0.85	-0.16
Rb					0.08

Figure 6. (**A**) Lithostratigraphy and selected geochemical variables for unit 2b. The thicker left curves for each element represents the normalized peaks (see text for explanation) and the thinner right curves for each element the peak area in counts/second/measuring point (kpcs). The Zr/Rb curve is a proxy for grain size variations. See Table 1 and Figure 3 for the stratigraphic legend. (**B**) Correlation matrices (*r* values) for selected elements of unit 2b.

run-off. This interpretation compares well to the record for core CP3A (Wohlfarth et al., 2012), where an increase in planktonic diatoms relative to benthic diatoms indicates an increase in water depth.

High organic matter and high organic carbon values suggest high lake organic productivity during the past 600 years. The C/N ratios together with $\delta^{13}C$ values signify a predominance of aquatic organic matter sources (cf. Meyers, 1997; Meyers and Teranes, 2001). However, the depleted $\delta^{15}N$ values could also suggest that N-fixing bacteria (cyanobacteria) may represent a significant proportion of the primary producers in the lake. The low BSi values compare well to the very low diatom percentages observed in this zone of CP3A (Wohlfarth et al., 2012) and to the disappearance of phytoliths in the upper part of the KUM.3 sequence (Kealhofer and Penny, 1998). Low element values indicate less contribution of mineral material. Changes in run-off and lower Si supply and/or changes in pH (suggested by higher Ca counts) could be one explanation for the low preservation of biogenic silica. Another explanation for the absence of biogenic silica could be competition with blue-green algae. The increase in %TN could be related to a higher proportion of cyanobacteria or to higher nutrient load from the catchment leading to higher productivity, which in turn could be related a change in land use and human activity (e.g., Hodell and Schelske, 1998; Matzinger et al., 2007).

6. Correlation of CP4 to other sediment sequences in Lake Kumphawapi

Several sediment sequences have previously been described from Lake Kumphawapi (Figure 1B). Kealhofer and Penny (1998) and Penny (1998, 1999) analyzed pollen and phytolith assemblages in sediment core KUM.3, which is located close to CP4, and provided an environmental reconstruction over the last 12,400 cal yr BP. Additional pollen stratigraphic studies used sediment core KUM.1, while KUM.2 was only analyzed for LOI and magnetic susceptibility (Penny, 1998, 1999). The published ^{14}C dates for these three sequences have recently been recalibrated (Wohlfarth et al., 2012). CP3A is located further to the north of CP4 and provides a c. 9400 year long record of past changes in lake status based on diatoms and geochemistry (Wohlfarth et al., 2012).

Seismic investigations in Kumphawapi in 2009 to assess sediment depth and lake bottom topography were unsuccessful due to the dense vegetation and the high organic content, but the difference in age for the sedimentary changes from lake to wetland in the different sequences suggests that Kumphawapi contains several sub-basins of varying depths (Figure 9). Sediments in shallower basins must have registered a change in water level and in moisture availability earlier than those from deeper sub-basins. The analysis of only one sediment sequence in a large lake such as Kumphawapi therefore may lead to erroneous estimates of past changes in water level and hydroclimate. The availability of multiple sediment sequences for Kumphawapi now allows for a better understanding of the basin topography of this large lake and provides a more detailed picture of the response to past climatic changes recorded in its sediments.

The clay loams and gyttja clays in the lower part of the sediment stratigraphy of KUM.3, KUM.2 and CP4, respectively, correlate well with each other in time. The chronology of all three sequences dates the deposition of these layers to older than c.

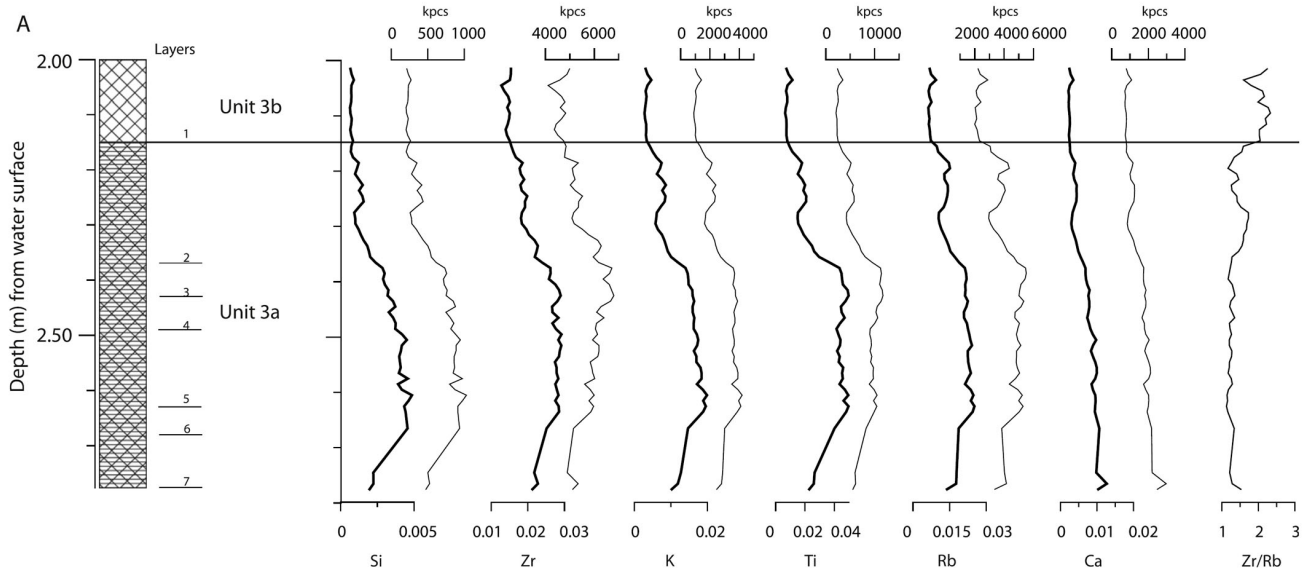

B

Unit 3a

	Zr	K	Ti	Rb	Ca
Si	0.66	0.96	0.89	0.84	0.76
Zr		0.73	0.86	0.80	0.38
K			0.95	0.92	0.77
Ti				0.93	0.65
Rb					0.62

Unit 3b

	Zr	K	Ti	Rb	Ca
Si	-0.01	0.62	0.70	0.51	0.61
Zr		-0.01	0.10	0.27	0.07
K			0.96	0.90	0.75
Ti				0.87	0.83
Rb					0.61

Figure 7. (**A**)Lithostratigraphy and selected geochemical variables for units 3a and 3b. The thicker left curves for each element represents the normalized peaks (see text for explanation) and the thinner right curves for each element the peak area in counts/second/measuring point (kpcs). The Zr/Rb curve is a proxy for grain size variations. See Table 1 and Figure 3 for the stratigraphic legend. (**B**) Correlation matrices (*r* values) for selected elements of unit 3a and 3b.

7200 cal yr BP (Figure 9). The lithological change from gyttja clay to clayey gyttja and peaty gyttja in CP4, from low organic to higher organic loam and peat in KUM.3, or from clay to peat in KUM.2 shows that parts of the lake had transformed into a wetland and that some areas had become a peatland shortly after c. 7200–7000 cal yr BP. Following the chronology of CP4, the wetland persisted until at least 6500 cal yr BP and then transformed into a peatland that underwent periodic desiccation, as seen by the long hiatus between 6500 and 1600 cal yr BP, and by intervals with higher contributions of mineral particles. No hiatus is reported for KUM.3 and KUM.2 (Kealhofer and Penny, 1998; Penny, 1998, 1999), but the ^{14}C dates for these two sequences do not contradict the presence of a hiatus in the peat either. In all three sediment sequences the re-establishment of a lake phase is dated to c. 1800–1500 cal yr BP (Figure 9).

Sediment sequences CP3A and KUM.1 further to the north show mineral-rich sediments in the bottom. In CP3A the gyttja clays grade into a sequence of gradually more organic sediments at c. 6700 cal yr BP, while a transition to peaty gyttja and peat is only seen at c. 5400 cal yr BP. Wohlfarth et al. (2012) argued that the transition from gyttja clay to clay gyttja at c. 6700 cal yr BP could signify reduced effective moisture. The clayey sediments in KUM.1 on the other hand are replaced by peat around 6000 cal yr BP, although the pollen stratigraphy shows that herbaceous swamp communities already started to develop around 7000 cal yr BP (Penny, 1998, 1999) (Figure 9). Proxies and hiatuses in the peat and in the peaty gyttja of CP3A (c. 5200–1600 cal yr BP) indicate the presence of more than one break in sedimentation (Figure 9). The basin where CP3A is located became flooded by the rise in lake level at c. 1600 cal yr BP, but the area around KUM.1 was not affected.

Wohlfarth et al. (2012) noted the age difference between CP3A and KUM.3 and KUM.2 for the transition from lake sediments to wetland/peat deposits and explained it as caused by errors in the KUM.3 chronology. However, the stratigraphy, geochemistry and chronology of CP4 now adds further knowledge and allows a discussion of the lithostratigraphic changes in a new perspective.

It is obvious that the lithostratigraphic change from clay and clayey gyttja sediments to peaty gyttja and peat occurred around 7200–7000 cal yr BP in the southern part of the lake. However, in the northern part of the lake, where KUM.1 and CP3A are situated, this transition occurred around 6000 and 5400 cal yr BP, respectively (Figure 9). This would imply that the bottom topography of the lake is highly variable and that different sub-basins can be differentiated, a southern shallow sub-basin (KUM.3, CP4 and KUM.2), a deeper northern sub-basin (CP3A) and a shallower basin further to the north (KUM.1). Climatic changes, such as a shift from wetter to drier conditions, would thus affect the sedimentation in the different sub-basins differently. The earliest signs of a shift to drier climatic conditions are seen in the sediments of KUM.3, CP4 and KUM.2 at around 7200–7000 cal yr BP, when the shallow lake in the southern part transformed into a wetland/peatland (Figure 9). No sedimentary change is seen at around 7000 cal yr BP in KUM.1, but pollen assemblages show an expansion of swamp communities (Penny, 1998, 1999), which would imply a lowering of the lake level. CP3A, on the other hand, displays a lithological change to more organic sediments around 6700 cal yr BP, which could have been initiated by a change in water level. The peat deposits in CP4 are characterized by a long-lasting hiatus (c. 6400–1600 cal yr BP), which shows that conditions had become too dry for continuous peat growth in the southern sub-basin. In

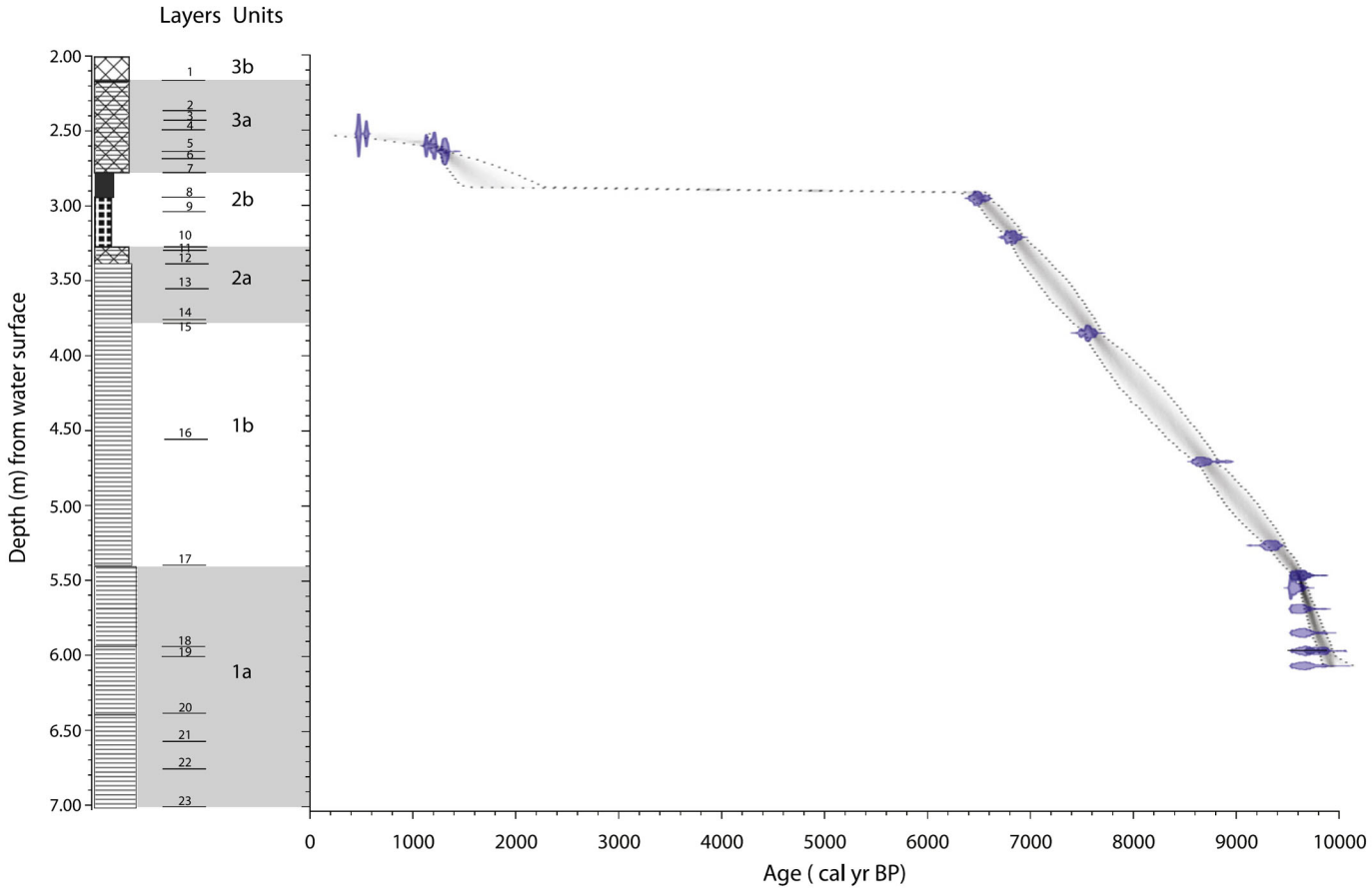

Figure 8. Lithostratigraphy of CP4 and modeled age–depth curve. The blue shapes show calibrated ^{14}C dates, the grey shading indicates the likely age-model and the dotted lines show the 95% confidence ranges. The dashed line between 6500 and 1300 cal yr BP marks the inferred hiatus. See Table 2 for details on the ^{14}C dates and Figure 3 for a stratigraphic legend.

contrast, the water level in the shallow part of the northern sub-basin (CP3A) gradually decreased after c. 6700 cal yr BP, and the basin transformed into a wetland/peatland at c. 5400 cal yr BP (Figure 9). The hiatus between c. 5200 and 4000 cal yr BP seen in the peat in CP3A moreover suggests severe dryness during this time interval. Around 3200 cal yr BP the water level increased slightly in the northern sub-basin (CP3A) and led to the re-establishment of a wetland (Wohlfarth et al., 2012). Multiple hiatuses in these wetland sediments, however, show that wetter and drier conditions alternated, which explains the long-lasting hiatus seen in CP4.

The transition from peatland/wetland to a new lake phase seems to have been more or less synchronous, since it is dated to approximately 1800–1500 cal yr BP in KUM.3, CP4, KUM.2 and CP3A. At the location of KUM.1, however, peat growth continued, which shows that the new lake had a smaller size than the lake that existed earlier.

7. Climatic and environmental interpretation of Lake Kumphawapi

Sediments dating to >10,000 cal yr BP were not attained in CP4. However, based on Kealhofer and Penny (1998) and Penny (1998, 1999), the catchment of Kumphawapi may have been composed of sparse dryland, grassy floodplain and backswamp vegetation communities (Figure 9). The subsequent diversification of arboreal taxa is interpreted as an expansion of dryland forests under more humid climatic conditions (Kealhofer and Penny, 1998). The geochemical proxies in CP4 suggest that Kumphawapi became an open water lake with high-energy sediment transport, high run-off and sparse and open vegetation around the shore >9800 cal yr BP. Weathering seems to have been considerable, likely as a consequence of higher precipitation, higher effective moisture and a stronger summer monsoon.

Less run-off and more stable lake conditions between c. 9600 and 7000 cal yr BP are indicated by the proxies analyzed in CP4. This interpretation compares well to that obtained from CP3A, where the different proxies indicated a shallow freshwater lake, and higher moisture availability for between c. 9400 and 6700 cal yr BP (Wohlfarth et al., 2012). Pollen stratigaphic data from KUM.3 for c. 9100 to 6800 cal yr BP suggest significant changes in the local flora (Penny, 1999), with marked increases in sedge pollen and fern spores (Figure 9). Phytolith assemblages show an increase in *Cyperaceae* and *Oryza* phytoliths, while Chloridoid and Panicoid grasses and bamboos decline significantly (Kealhofer and Penny, 1998). This development was interpreted as an increase in water level, i.e., as a hydrological change in the basin and consequently as a period of higher moisture availability (Kealhofer and Penny, 1998), which is in line with the interpretation of CP4 and CP3A.

The change in sediment lithology and geochemistry in CP4 around 7100–7000 cal yr BP give evidence for a distinct shift in lake status from an open, shallow lake to a wetland. The increasing organic content of the sediments, lower sediment accumulation rates, and higher terrestrial organic matter content characterize this transition and show that run-off decreased considerably. A lowering of the lake level, a further development of herbaceous swamp communities and a reduction in dryland taxa in the lake's catchment around 7000 cal yr

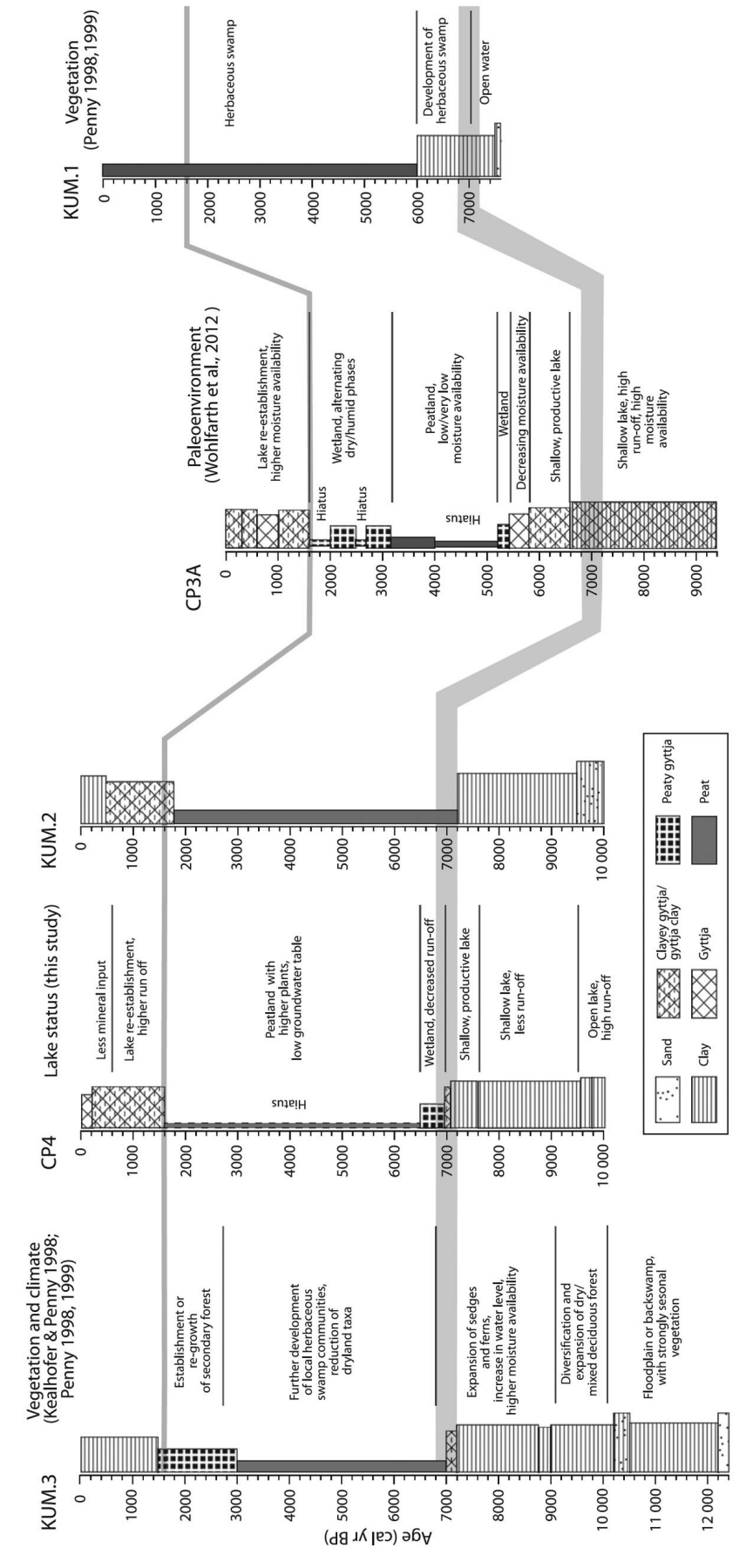

Figure 9. Correlation of CP4 to other studied sediment sequences in Kumphawapi: KUM.3, KUM.2, KUM.1 (Kealhofer and Penny, 1998; Penny, 1998, 1999) and CP3A (Wohlfarth et al., 2012). See Figure 1B for the location of the coring points. The calibrated ages for KUM.3, KUM.2 and KUM.1 are according to Wohlfarth et al. (2012).

BP have been noted by Kealhofer and Penny (1998) and Penny (1999) for KUM.3. These observations compare well to the lake status changes observed in CP4. Together, this can be interpreted as a reduction in moisture availability and possibly as a weakening of the summer monsoon. The sediments and the geochemical proxies in CP3A show an increase in organic content around 6700 cal yr BP and a change to a shallow, high productivity lake, which could also be interpreted as signifying less effective moisture (Wohlfarth et al., 2012). The lowering of the lake level and the start of drier conditions obviously affected the shallower basin by around 7000 cal yr BP, while the deeper parts still contained a shallow water body, which, as moisture availability decreased, only dried out later.

Sometime after 6500 cal yr BP the southern sub-basin with KUM.3, CP4 and KUM.2 transformed from a wetland into a peatland (Figure 9). In CP4 this transition coincides with a hiatus. Geochemical proxies indicate organic matter from higher plants, which probably colonized the peat surface, and $\delta^{34}S$ values would suggest a lowering of the groundwater table. Changes in elemental proxies and %TOC between 2.93 and 2.88 m depth in CP4, which suggest periodic dryness of the peat surface, might correlate with the high concentration of charcoal, which has been observed in KUM.3 (Kealhofer and Penny, 1998; Penny, 1998, 1999). White et al. (2004) discussed whether the high amounts of charcoal could be the result of natural forest fires due to a drier climate, or whether these indicate human activities, which also led to a reduction in forests within the catchment. While the southern sub-basin had dried out sometime after 6500 cal yr BP, the northern sub-basin with CP3A still contained a shallow lake. The water level only started to drop at c. 5900 cal yr BP, and the shift to a wetland with predominantly terrestrial vegetation occurred c. 5400 cal yr BP (Wohlfarth et al., 2012). The fact that the southern sub-basin transformed from a shallow lake to a wetland and subsequently to a peatland suggests a decrease in effective moisture by around 7000 cal yr BP. However the sediments in the deeper northern sub-basin did not register the shift from lake to wetland and peatland until c. 5900 cal yr BP and 5400 cal yr BP, respectively. One could speculate that climatic conditions had become very dry after 5400 cal yr BP, and that the low groundwater level made it impossible to maintain a shallow lake also in the northern part. Indeed, the stratigraphy of CP3A indicates an interval of severe dryness between 5200 and 4000 cal yr BP (Wohlfarth et al., 2012).

Following the chronology and the pollen stratigraphy for KUM.3, the peatland existed until c. 3000 cal yr BP, when it transformed again into a wetland (Kealhofer and Penny, 1998, Figure 9). This transition compares well to CP3A, where the change from peat to wetland is dated to c. 3200 cal yr BP (Wohlfarth et al., 2012). Although a long hiatus is present in CP4 and prevents an age assignment for the peat, one could assume that the transition from peat to wetland occurred at about the same time. This shift would signify a rise in water level and flooding of the peat surface as a consequence of higher effective moisture. However, as shown by CP3A, two intervals with reduced effective moisture characterize this wetland phase, one at c. 2700–2500 cal yr BP and another between c. 1900 and 1600 cal yr BP.

The start of the second lake phase and a higher water level in the Kumphawapi basin at c. 1600 cal yr BP coincides with the end of the hiatus in CP4 and also with a hiatus in CP3A. $\delta^{34}S$ values in CP4 suggest a rise in the groundwater table, and diatom assemblages in CP3A testify for an increase in water depth. Higher effective moisture and a stronger summer monsoon might account for the renewed filling of the basin. On the other hand, geochemical proxies in CP4 could provide evidence for anthropogenic activities in the catchment after 600 cal yr BP. Although archaeological remains around Kumphawapi are poorly dated, boundary stones from the Ban Don Kaeo peninsula (Figure 1B) date settlements there to c. 800 AD (Penny, 1999) or 1150 cal yr BP.

8. Correlation to other Asian monsoon records

The sedimentary records and their proxies in Kumphawapi imply higher precipitation >10,000 to c. 7000 cal yr BP, likely caused by a stronger summer monsoon. Lake status and water level changes around 7000 cal yr BP suggest a shift to less effective moisture. By 6500 cal yr BP parts of the large lake had transformed into a peatland, while shallow water bodies still occupied the deeper basin until c. 5200 cal yr BP. This development indicates that effective moisture had decreased, possibly as a result of a gradually weaker summer monsoon. As shown by the comparison of multiple sediment sequences in Lake Kumphawapi (Figure 9), the interval between c. 5200 and 3200 cal yr BP seems to have been the driest interval in Kumphawapi's history. Thereafter, the water level increased, which led to the formation of a wetland in the deeper parts. This wetland existed until c. 1600 cal yr BP and experienced episodes of severe dryness around c. 2700–2500 and 2000–1600 cal yr BP (Wohlfarth et al., 2012). The alternation between wet and dry episodes may indicate a strengthened summer monsoon and intervals with a distinctly weaker summer monsoon.

Kumpawapi's record can be compared to other paleoclimate data sets from the Asian monsoon region (Figure 10). The regionally nearest records are from northwest Thailand (Marwick and Gagan, 2011) and Cambodia (Maxwell, 2001; Penny, 2006). $\delta^{18}O$ values on freshwater bivalves from the Tham Lod and Ban Rai rock shelters (Figure 10) suggest high precipitation until 9800 cal yr BP and a subtle trend towards drier conditions until c. 5900 cal yr BP (Marwick and Gagan, 2011). A stronger summer monsoon between 9500 and 6200 cal yr BP and drier conditions between 6200 and 2700 cal yr BP are reconstructed for Lake Kara in Cambodia (Figure 10) (Maxwell, 2001). The sedimentary record of Tonle Sap (Figure 10), also in Cambodia, shows strong variations in seasonal rainfall between 7800 and 5800 cal yr BP, and a decrease in rainfall and increased seasonality since the mid-Holocene (Penny, 2006). The early Holocene interval of stronger effective moisture availability inferred from the Kumphawapi sequence is comparable in time to these records, although a decrease in effective moisture availability is registered in Kumphawapi by c. 7000 cal yr BP, and severe dry condition seem to have prevailed between c. 5200 and 3200 cal yr BP.

$\delta^{18}O$ speleothem records from Dongge Cave in southwestern China (Figure 10) suggest that the Southwest Asian summer monsoon was stronger between 9000 and 7000 cal yr BP and then declined in a stepwise manner. Dykoski et al. (2005) noted a marked shift in summer monsoon intensity around 5600 and 3500 cal yr BP, and Wang et al. (2005a) proposed a series of short-term weak summer monsoon events, which were superimposed on the general trend of decreasing summer monsoon intensity (8300, 7200, 6300, 5500, 4400, 2700, 1600, and 500 cal yr BP). The pollen record from Lake Huguang Maar in southern China (Figure 10) suggests high moisture availability between 11,600 and 7800 cal yr BP, lower temperatures and humidity between 7800 and 4200 cal yr BP, and a marked decrease in temperature and humidity between 4200 and 350 cal yr BP (Wang et al., 2007). However, multi-proxies from the same lake suggest that the strong early Holocene summer monsoon began to decline at 6080 cal yr BP, which is c. 1700 years later than the earlier estimate, and that it has been weak since 3600 cal yr BP (Wu et al., 2012). $\delta^{18}O$ records from Lakes Xingyun and Qili in southwest China (Figure 10) also indicate an intensified summer monsoon during the early Holocene, but its gradual weakening seems to have started al-

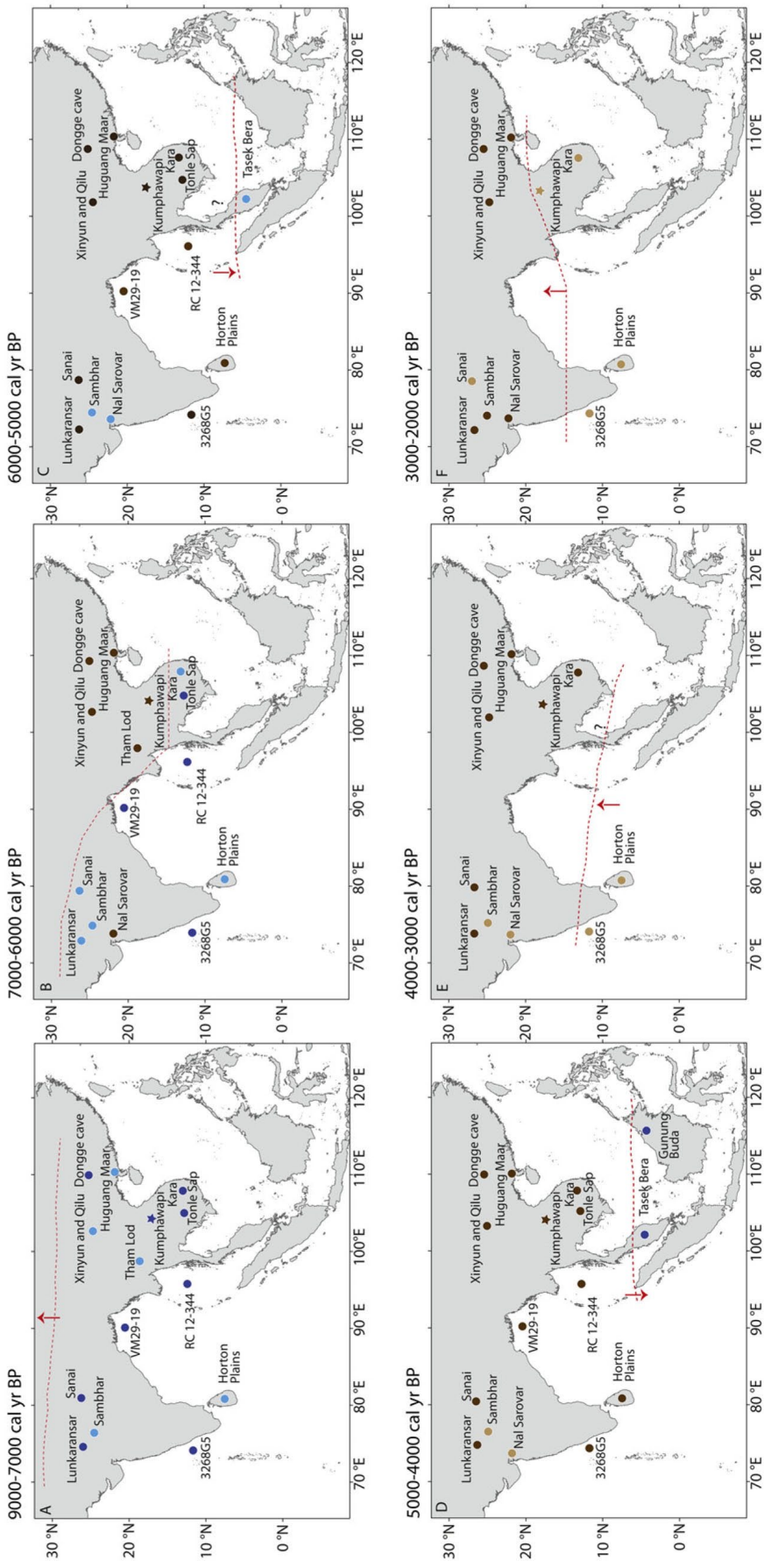

Figure 10. (**A–F**) Spatial and temporal variability of the Asian summer monsoon during the Holocene reconstructed from marine and terrestrial records. Lake sediment and peat records: Lake Kara (Maxwell, 2001); Tonle Sap (Penny, 2006); Huguang maar (Wang et al., 2007; Wu et al., 2012); lakes Xingyun and Qilu (Hodell et al., 1999), Lunkaransar (Enzel et al., 1999); Sambhar (Sinha et al., 2006); Sanai, Ganga Plain (Sharma et al., 2004); Nal Sarovar (Prasad et al., 1997); Horton plains (Premathilake and Risberg, 2003); Tasek Bera basin (Wüst and Bustin, 2004). Cave sediment record: Tham Lod (Marwick and Gagan, 2011). Speleothem records: Gunung Buda (Partin et al., 2007), Dongge cave (Dykoski et al., 2005; Wang et al., 2005a). Marine records: RC 12-344 Andaman sea (Rashid et al., 2007); VM29-19 Bay of Bengal (Rashid et al., 2011); 3268G5 Arabian sea (Sarkar et al., 2000). Dark blue filled circles = sites where low effective evaporation has been reconstructed; light blue filled circles = decreasing humidity; dark brown filled circles = high effective evaporation; light brown filled circles = increasing humidity. Red dashed line = reconstructed mean position of the ITCZ during the Holocene based on the above cited paleoclimatic records; arrows = movement direction of the ITCZ.

ready by around 8000 cal yr BP (Hodell et al., 1999). The short-term events of weak summer monsoon intensity at Dongge Cave are not visible in the Kumphawapi sequences, but the gradual decline in summer monsoon intensity in the Dongge record at 7000 cal yr BP is consistent with the lake level lowering and inferred lower effective moisture availability for Kumphawapi. Also, the marked shift in summer monsoon intensity around 5600 cal yr BP in the Dongge record (Dykoski et al., 2005) is close to the start of severe dry conditions seen in Kumphawapi at c. 5200 cal yr BP. However the second distinct shift in the Dongge record at 3500 cal yr BP is less clear in Kumphawapi, where wet and dry intervals seem to have alternated between 3200 and 1600 cal yr BP. The observed lake-level rise in Kuphawapi after 1600 cal yr BP explained by higher moisture availability is also not consistent with short-term weak summer monsoon events in the Dongge record. The shift to a weaker summer monsoon inferred for around 7000 cal yr BP in Dongge cave and Kumphawapi occurred slightly later than that assumed for Lakes Huguang Maar (7800 cal yr BP), Xingyun and Qili (8000 cal yr BP). Older ages for this shift in Lakes Xingyun and Qili could have been caused by a hard-water effect (Zhang et al., 2011). In contrast, lacustrine records in the Badain Jaran Desert of western Inner Mongolia (China), which is located along the northern margin of the EASM, suggest that summer monsoons were stronger between 10000 and 4000 cal yr BP, causing wetter climatic conditions in this mid-latitude desert region (Yang et al., 2010, 2011). However along the eastern side of the desert belt, paleosols and Aeolian sands indicate that the EASM maximum was restricted to 6000–4000 cal yr BP (Yang et al., 2008).

Marine Mg/Ca and $\delta^{18}O$ records from the Andaman Sea and the western Bay of Bengal (Figure 10) provide sea-surface temperature and salinity estimates (Rashid et al., 2007, 2011). Increased river run-off and a stronger Indian summer monsoon are reconstructed for the early Holocene, whereas a weakening of the summer monsoon is recognized after c. 5600–5500 cal yr BP. $\delta^{18}O$ data series from the eastern Arabian Sea (Figure 10) suggest significant spatial variability in Holocene monsoon rainfall, alternatively higher precipitation during the early Holocene, arid conditions between 6000 and 3500 cal yr BP and higher precipitation again between 3500 and 2000 cal yr BP (Sarkar et al., 2000). The intensified early Holocene summer monsoon inferred from these records is comparable to the interval of high effective moisture availability seen in Kumphawapi. The mid-Holocene weakening of the summer monsoon between c. 6000 and 5600 cal yr BP also compares well to the beginning of dry conditions in Kumphawapi. However, the marine records do not seem to register the start of a gradually weaker summer monsoon around 7000 cal yr BP.

Lake-level studies in the Thar Desert of Northwest India (Figure 10) provide slightly different pictures for the two lakes, Lunkaransar (Enzel et al., 1999) and Sambhar (Sinha et al., 2006). Lunkaransar's lake level was low and fluctuating during the early Holocene. It attained a maximum around 7200 cal yr BP and dropped around 6000 cal yr BP. The lake had dried out completely by 5500 cal yr BP. The Lake Sambhar sediment sequence, on the other hand, indicates lake-level fluctuations and moderate precipitation during the early Holocene, which were followed by an arid phase between 7500 and 6500 cal yr BP. Lake expansion between 6500 and 3000 cal yr BP is interpreted as reflecting higher effective moisture, and the disappearance of the lake after 3000 cal yr BP as indicating a semi-arid climate (Sinha et al., 2006). Geochemistry and vegetation reconstructions from Sanai Lake in northern India (Figure 10) indicate high moisture availability until ca. 6500 cal yr BP, arid conditions c. 6500–2300 cal yr BP and an increase in effective moisture availability after c. 1600 cal yr BP (Sharma et al., 2004). $\delta^{13}C$ and C/N records from Lake Nal Sarovar in western India (Figure 10) suggest a drier period between 7600 and 5000 cal yr BP, a wetter interval between 5000 and 3300 cal yr BP and an increase in aridity after 3000 cal yr BP (Prasad et al., 1997). The early Holocene strong summer monsoon reconstructed for India is comparable in time to paleoclimate reconstructions from Indochina and Southern China. However, the timing of the initiation of a weaker summer monsoon and dry periods varies significantly among sites in India and is accordingly difficult to compare to records from Indochina and China. A better chronological framework for the Indian sites is needed to assess whether this seemingly time-transgressive pattern of summer monsoon weakening is real or due to, e.g., differences in geography and in the proxies used for paleoclimatic reconstruction.

High-resolution pollen records from the Horton Plains on central Sri Lanka (Figure 10) suggest marked humidity during the early Holocene, increasing aridity around 8500 cal yr BP, semi-arid climatic conditions between 5500 and 3500, humid conditions between 3500 and 2000, and fluctuating climates after 2000 cal yr BP (Premathilake and Risberg, 2003). Interestingly, the effective moisture reconstructed for Sri Lanka compares well with Kumphawapi's history, although aridity seems to have increased c. 1000 earlier on Sri Lanka.

The complex stratigraphic peat records of the Tasek Bera Basin in Malaysia (Figure 10) show the start of a series of rapid hydrologic changes around 6000 cal yr BP (Wüst and Bustin, 2004), which is in agreement with increasingly wet conditions peaking at c. 5000 cal yr BP on northwestern Borneo (Figure 10) (Partin et al., 2007). The distinct mid-Holocene precipitation peak observed in the Malayan-Borneo records is dissimilar to Indochina, Southern China and India. Monsoon precipitation seems to have increased in areas close to the equator (Malaysia, Borneo) and in the desert areas along the northern margin of the EASM, but decreased in areas located at the middle of the pathway of the Asian summer monsoon domain (Southern China and Indochina). This would imply a southward shift in the mean position of the ITCZ (e.g. Fleitmann et al., 2007; Yancheva et al., 2007; Griffiths et al., 2009), which would have resulted in high precipitation over Malaysia and Indonesia during the middle Holocene, but in dry conditions over Indochina and China.

The time-slices in Figure 10A–E present a fairly coherent picture of Asian monsoon variability during the Holocene. The time interval between 9000 and 7000 cal yr BP displays wet conditions for most records, but also that humidity started to decrease (e.g., Tham Rod, Huguang Maar, Xinyun, Qilu and Horton plains) (Figure 10A). Between 7000 and 3000 cal yr BP, less moisture and dry conditions prevailed at most of the sites north of 5°N, which suggests a southward shift in the mean position the ITCZ and as such a weaker summer monsoon (Figure 10B–E). The exceptions are the three marine sites, which show wetter conditions until 6000 cal yr BP, and the two lakes Sambhar and Nal Sarovar in Northwest India, which seem to register wetter conditions by 6000 cal yr BP. Regional climate and hydrology may be a major factor in determining the ecological response to climate change and/or different proxies used for climate reconstruction could cause apparent time lags or gradual responses. Between 4000 and 3000 cal yr BP, records from the Horton Plains on Sri Lanka and from the eastern Arabian Sea again suggest higher effective moisture, whereas other records still display dry conditions. However, between 3000 and 2000 cal yr BP records from Indochina also point to higher moisture availability, comparable to those from Sri Lanka and the eastern Arabian Sea (Figure 10E–F). This could indicate that the northern boundary of the ITCZ had moved farther north. The gradual decrease of the summer monsoon together with a southward shift in the mean position of the ITCZ between c. 7000 and 4000 cal yr

BP seems to be synchronous in most of the records from Indochina, Southern China and Sri Lanka, while the opposite is the case for northwest India. However, more paleoclimatic records between 5 and 15°N, for example from southern Thailand, and from southern and central India, need to be investigated to discuss the shift in the mean position of the ITCZ between 4000 and 2000 cal yr BP in greater detail.

Although a wealth of high-resolution paleo-precipitation records exist for the past 1000 years (Cook et al., 2010), these are difficult to compare to the low-resolution data sets discussed here. The late Holocene lake-level rise in Kumphawapi, along with inferred higher moisture availability needs to be constrained by a better chronology to enable for example comparisons to regional tree-ring records, and to decipher whether the changes seen in Kumphawapi were caused by human influence or whether these were due to climatic factors. More high-resolution and multi-proxy paleoenvironmental, paleoclimatic and archaeological data for Thailand and for the Asian monsoon region are needed to assess in greater detail the spatial and temporal variability of the Asian monsoon during the Holocene.

9. Conclusions

The availability of multiple sediment sequences and proxies from Lake Kumphawapi in northeast Thailand allows for a better understanding of how basin topography influences sediment deposition in this large lake, and provides a more detailed picture of the lake's response to past climatic changes. The sediment sequences and their proxies suggest a strong summer monsoon between c. 9800 and 7000 cal yr BP. Effective moisture seems to have decreased after 7000 cal yr BP, as seen by the gradual transformation from lake to wetland. The reconstruction of driest conditions between 5200 and 3200 cal yr BP compares well with other paleoarchives from the Asian monsoon region. After 3200 cal yr BP, the deepest part of the lake turned into a wetland, while shallower areas remained dry. By 1600 cal yr BP a lake had become re-established in the basin, but this lake had a smaller size than the lake that existed before. Kumphawapi's record provides the first comprehensive paleoclimatic and paleoenvironmental synthesis for northeast Thailand during the Holocene. It suggests a gradual decrease of the summer monsoon and a southward shift in the mean position of the ITCZ between c. 7000 and 3000 cal yr BP. The ITCZ possibly moved northward again after 3000 cal yr BP. The detailed paleoclimatic information derived from Kumphawapi provides important baseline information for reconstructing Holocene monsoon variability, ITCZ movement, and model-data comparisons.

Acknowledgments — We thank the Stable Isotope Laboratory at the Department of Geological Sciences, Stockholm University and Heike Sigmund for analyzing total and CNS isotopes, Hildred Crill for English language assistance, and Thanawat Jarupongsakul and Suda Inthongkaew for logistic support during fieldwork. Research in Thailand is financed through Swedish Research Council (VR) research grants 621-2008-2855 and 348-2008-6071. S. Chawchai acknowledges financial support from the Royal Thai Government Scholarship under DPST project for her PhD study.

References

An, Z., Porter, S.C., Kutzbach, J.E., Xihao, W., Suming, W., Xiaodong, L., Xiaoqiang, L., Weijian, Z., 2000. A synchronous Holocene optimum of the East Asian monsoon. *Quaternary Science Reviews* 19, 743–762.

Blaauw, M., Christen, J.A., 2011. Flexible paleoclimate age-depth models using an autoregressive gamma process. *Bayesian Analysis* 6, 457–474.

Boyd, W.E., 2008. Social change in late Holocene mainland SE Asia: A response to gradual climate change or a critical climatic event? *Quaternary International* 184, 11–23.

Brenner, M., Whitmore, T.J., Curtis, J.H., Hodell, D.A., Schelske, C.L., 1999. Stable isotope ($\delta^{13}C$ and $\delta^{15}N$) signatures of sedimented organic matter as indicators of historic lake trophic state. *Journal of Paleolimnology* 22, 205–221.

Buckley, B.M., Palakit, K., Duangsathaporn, K., Sanguantham, P., Prasomsin, P., 2007. Decadal scale droughts over northwestern Thailand over the past 448 years: Links to the tropical Pacific and Indian Ocean sectors. *Climate Dynamics* 29, 63– 71.

Cai, B., Pumijumnong, N., Tan, M., Muangsong, C., Kong, X., Jiang, X., Nan, S., 2010. Effects of intraseasonal variation of summer monsoon rainfall on stable isotope and growth rate of a stalagmite from northwestern Thailand. *Journal of Geophysical Research* 115, D21104.

Chen, F., Yu, Z., Yang, M., Ito, E., Wang, S., Madsen, D.B., Huang, X., Zhao, Y., Sato, T., Birks, John B.H., Boomer, I., Chen, J., An, C., Wünnemann, B., 2008. Holocene moisture evolution in arid central Asia and its out-of-phase relationship with Asian monsoon history. *Quaternary Science Reviews* 27, 351–364.

Conley, D.J., 1998. An interlaboratory comparison for the measurement of biogenic silica in sediments. *Marine Chemistry* 63, 39–48.

Conley, D.J., Schelske, C.L., 2001. Biogenic silica. In: Smol, J.P. (ed.), *Tracking Environmental Change Using Lake Sediments: Terrestrial, Algal, and Siliceous Indicators.* Kuwer Academic, Dordrecht, The Netherland, pp. 281–293.

Cook, C.G., Jones, R.T., 2012. Palaeoclimate dynamics in continental Southeast Asia over the last ~30,000 cal yrs BP. *Palaeogeography, Palaeoclimatology, Palaeoecology* 339–441, 1–11.

Cook, E.R., Anchukaitis, K.J., Buckley, B.M., D'Arrigo, R.D., Jacoby, G.C., Wright, W.E., 2010. Asian monsoon failure and megadrought during the last millennium. *Science* 328, 486–489.

Corella, J.P., Amrani, A.E., Sigró, J., Morellón, M., Rico, E., Lorenzo, B., Garcés, V., 2010. Recent evolution of Lake Arreo, northern Spain: Influences of land use change and climate. *Journal of Paleolimnology* 46, 469–485.

Department of Mineral Resources (DMR), 2009. Geological Map of Changwat Udon Thani, Scale 1:250,000.

de Vries, H., Barendsen, G.W., 1952. A new technique for the measurement of age by radiocarbon. *Physica* 18, 652.

Dykoski, C., Edwards, R., Cheng, H., Yuan, D., Cai, Y., Zhang, M., Lin, Y., Qing, J., An, Z., Revenaugh, J., 2005. A high-resolution, absolute-dated Holocene and deglacial Asian monsoon record from Dongge Cave, China. *Earth and Planetary Science Letters* 233, 71–86.

Dypvik, H., Harris, N.B., 2001. Geochemical facies analysis of fine grained siliciclastics using Th/U, Zr/Rb and (Zr+Rb)/Sr ratios. *Chemical Geology* 181, 131–146.

El Tabakh, M., Utha-Aroon, C., Schreiber, B.C., 1999. Sedimentology of the Cretaceous Maha Sarakham evaporites in the Khorat Plateau of northeastern Thailand. *Sedimentary Geology* 123, 31–62.

El Tabakh, M., Utha-Aroon, C.,Warren, J.K., Schreiber, B.C., 2003. Origin of dolomites in the Cretaceous Maha Sarakham evaporites of the Khorat Plateau, northeast Thailand. *Sedimentary Geology* 157, 235–252.

Enzel, Y., Ely, L.L., Mishra, S., Ramesh, R., Amit, R., Lazar, B., Rajaguru, S.N., Baker, V.R., Sandler, A., 1999. High-resolution Holocene environmental changes in the Thar desert, northwestern India. *Science* 284, 125–128.

Fleitmann, D., Burns, S.J., Mangini, A., Mudelsee, M., Kramers, J., Villa, I., Neff, U., Al- Subbary, A.A., Buettner, A., Hippler, D., Matter, A., 2007. Holocene ITCZ and Indian monsoon dynamics recorded in stalagmites from Oman and Yemen (Socotra). *Quaternary Science Reviews* 26, 170–188.

Fry, B., 2006. *Stable Isotope Ecology*. Springer, New York, 308 pp.

Griffiths, M.L., Drysdale, R.N., Gagan, M.K., Zhao, J.x., Ayliffe, L.K., Hellstrom, J.C., Hantoro, W.S., Frisia, S., Feng, Y.x., Cartwright, I., Pierre, E.S., Fischer, M.J., Suwargadi, B.W., 2009. Increasing Australian–Indonesian monsoon rainfall linked to early Holocene sea-level rise. *Nature Geoscience* 2, 636–639.

Herzschuh, U., 2006. Palaeo-moisture evolution in monsoonal Central Asia during the last 50,000 years. *Quaternary Science Reviews* 25, 163–178.

Hodell, D.A., Brenner, M., Kanfoush, S.L., Curtis, J.H., Stoner, J.S., Xueliang, S., Yuan, W., Whitmore, T.J., 1999. Paleoclimate of Southwestern China for the past 50,000 yr inferred from lake sediment records. *Quaternary Research* 52, 369–380.

Hodell, D.A., Schelske, C.L., 1998. Production, sedimentation, and isotopic composition of organic matter in Lake Ontario. *Limnology and Oceanography* 43, 200–214.

Kealhofer, L., Penny, D., 1998. A combined pollen and phytolith record for fourteen thousand years of vegetation change in northeastern Thailand. *Review of Palaeobotany and Palynology* 103, 83–93.

Klubseang, W., 2011. Paleogeography and Paleoenvironment of Nong Han Kumphawapi, Changwat Udon Thani. Chulalongkorn University, Bangkok, 110 pp., MSc thesis.

Kutzbach, J.E., 1981. Monsoon climate of the Early Holocene: Climate experiment with the Earth's orbital parameters for 9000 years ago. *Science* 214, 59–61.

Kylander, M.E., Ampel, L., Wohlfarth, B., Veres, D., 2011. High-resolution X-ray fluorescence core scanning analysis of Les Echets (France) sedimentary sequence: New insights from chemical proxies. *Journal of Quaternary Science* 26, 109–117.

Marwick, B., Gagan, M.K., 2011. Late Pleistocene monsoon variability in northwest Thailand: An oxygen isotope sequence from the bivalve *Margaritanopsis laosensis* excavated in Mae Hong Son province. *Quaternary Science Reviews* 30, 3088–3098.

Matzinger, A., Schmid, M., Veljanoska-Sarafiloska, E., Patceva, S., Guseska, D., Wagner, B., Müller, B., Sturm, M., Wüest, A., 2007. Eutrophication of ancient Lake Ohrid: Global warming amplifies detrimental effects of increased nutrient inputs. *Limnology and Oceanography* 52, 338–353.

Maxwell, A.L., 2001. Holocene monsoon changes inferred from lake sediment pollen and carbonate records, northeastern Cambodia. *Quaternary Research* 56, 390– 400.

Meyers, P.A., 1997. Organic geochemical proxies of paleoceanographic, paleolimnologic, and paleoclimatic processes. *Organic Geochemistry* 27, 213–250.

Meyers, P.A., Teranes, J.L., 2001. Sediment organic matter. In: Last, W.M., Smol, J.P. (eds.), *Tracking Environmental Change Using Lake Sediments: Physical and Geochemical Methods,* pp. 239–269. Dordrecht, The Netherland.

Morrill, C., Overpeck, J.T., Cole, J.E., 2003. A synthesis of abrupt changes in the Asian summer monsoon since the last deglaciation. *The Holocene* 13, 465–476.

Mortlock, R.A., Froelich, P.N., 1989. A simple method for the rapid determination of biogenic opal in pelagic marine sediments. *Deep Sea Research Part A. Oceanographic Research Papers* 36, 1415–1426.

Partin, J.W., Cobb, K.M., Adkins, J.F., Clark, B., Fernandez, D.P., 2007. Millennial-scale trends in west Pacific warm pool hydrology since the Last Glacial Maximum. *Nature* 449, 452–455.

Penny, D., 1998. Late Quaternary Palaeoenvironments in the Sakon Nakhon Basin, North-east Thailand. Monash University, Victoria, Australia, 260 pp., PhD thesis.

Penny, D., 1999. Palaeoenvironmental analysis of the Sakon Nakhon Basin, northeast Thailand: Palynological perspectives on climate change and human occupation. *Bulletin of the Indo-pacific Prehistory Association* 18, 139–149.

Penny, D., 2006. The Holocene history and development of the Tonle Sap, Cambodia. *Quaternary Science Reviews* 25, 310–322.

Prasad, S., Kusumgar, S., Gupta, S.K., 1997. A mid to late Holocene record of paleoclimatic changes from Nal Sarovar: A palaeodesert margin lake in western India. *Journal of Quaternary Science* 12, 153–159.

Premathilake, R., Risberg, J., 2003. Late Quaternary climate history of the Horton plains, central Sri Lanka. *Quaternary Science Reviews* 22, 1525–1541.

Rashid, H., England, E., Thompson, L., Polyak, L., 2011. Late Glacial to Holocene Indian summer monsoon variability based upon sediment records taken from the Bay of Bengal. *Terrestrial Atmospheric and Oceanic Science* 22, 215–225.

Rashid, H., Flower, B.P., Poore, R.Z., Quinn, T.M., 2007. A ~25ka Indian Ocean monsoon variability record from the Andaman Sea. *Quaternary Science Reviews* 26, 2586–2597.

Reimer, P.J., Baillie, M.G.L., Bard, E., Bayliss, A., Beck, J.W., Blackwell, P.G., Ramsey, C.B., Buck, C.E., Burr, G.S., Edwards, R.L., Friedrich, M., Grootes, P.M., Guilderson, T.P., Hajdas, I., Heaton, T.J., Hogg, A.G., Hughen, K.A., Kaiser, K.F., Kromer, B., McCormac, F.G., Manning, S.W., Reimer, R.W., Richards, D.A., Southon, J.R., Talamo, S., Turney, C.S.M., van der Plicht, J., Weyhenmeyer, C.E., 2009. IntCal09 and Marine09 radiocarbon age calibration curves, 0–50,000 years cal BP. *Radiocarbon* 51, 1111–1150.

Saccone, L., Conley, D.J., Sauer, D., 2006. Methodologies for amorphous silica analysis. *Journal of Geochemical Exploration* 88, 235–238.

Sarkar, A., Ramesh, R., Somayajulu, B.L.K., Agnihotri, R., Jull, A.J.T., Burr, G.S., 2000. High resolution Holocene monsoon record from the eastern Arabian Sea. *Earth and Planetary Science Letters* 177, 209–218.

Satarugsa, P., Meesawat, N., Thongman, W., Yangmee, W., 2004. Evaluation of natural hazard from a collapse of subsurface rock salt cavity in the northeastern Thailand (in Thai): Case studies from Nong Han Kumpawapee lake, Changwat Udon Thanee and Nong Bo reservoir Amphoe Borabue, Changwat Mahasarakam. *Khon Kaen University Research Journal* 9, 48–60.

Sattayarak, N., 1985. Northeast geology. In: *Proceedings of Conference on Geology and Minerals Resources Development of the Northeast, Thailand* (in Thai). Department of Geology, Khon Kaen University, pp. 23–30.

Sharma, S., Joachimski, M., Sharma, M., Tobschall, H., Singh, I., Sharma, C., Chauhan, M., Morgenroth, G., 2004. Late-glacial and Holocene environmental changes in Ganga plain, Northern India. *Quaternary Science Reviews* 23, 145–159.

Sinha, R., Smykatz-Kloss, W., Stüben, D., Harrison, S.P., Berner, Z., Kramar, U., 2006. Late Quaternary paleoclimatic reconstruction from the lacustrine sediments of the Sambhar playa core, Thar Desert margin, India. *Palaeogeography, Palaeoclimatology, Palaeoecology* 233, 252–270.

Slota, P.J., Jull, A.J.T., Linick, T.W., Toolin, L.J., 1987. Preparation of small samples for C-14 accelerator targets by catalytic reduction of Co. *Radiocarbon* 29, 303–306.

Stuiver, M., Polach, H.A., 1977. Discussion: reporting of 14C data. Radiocarbon 19, 355–363.

Vogel, J.S., Southon, J.R., Nelson, D.E., Brown, T.A., 1984. Performance of catalytically condensed carbon for use in accelerator mass-spectrometry. *Nuclear Instruments & Methods in Physics Research Section B* 233, 289–293.

Wang, P., Clemens, S., Beaufort, L., Braconnot, P., Ganssen, G., Jian, Z., Kershaw, P., Sarnthein, M., 2005. Evolution and variability of the Asian monsoon system: State of the art and outstanding issues. *Quaternary Science Reviews* 24, 595– 629.

Wang, S., Lü, H., Liu, J., Negendank, J.F.W., 2007. The early Holocene optimum inferred from a high-resolution pollen record of Huguangyan Maar Lake in southern China. *Chinese Science Bulletin* 52, 2829–2836.

Wang, Y., Cheng, H., Edwards, R.L., He, Y., Kong, X., An, Z., Wu, J., Kelly, M.J., Dykoski, C.A., Li, X., 2005a. The Holocene Asian Monsoon: Links to solar changes and North Atlantic climate. *Science* 308, 854–857.

Wang, Y., Liu, X., Herzschuh, U., 2010. Asynchronous evolution of the Indian and East Asian Summer Monsoon indicated by Holocene moisture patterns in monsoonal central Asia. *Earth-science Reviews* 103, 135–153.

Wannakomol, A., 2005. Soil and Groundwater Salinization Problems in the Khorat Plateau, NE Thailand – Integrated Study of Remote Sensing, Geophysical and Field Data. Freie Universität Berlin, Berlin, 198 pp., PhD thesis.

Warren, J.K., 1989. *Evaporite Sedimentology*. Prentice Hall, New Jersey, 285 pp.

White, J.C., Penny, D., Kealhofer, L., Maloney, B., 2004. Vegetation changes from the late Pleistocene through the Holocene from three areas of archaeological significance in Thailand. *Quaternary International* 113, 111–132.

Wohlfarth, B., Wichuratree, K., Inthongkaew, S., Fritz, S.C., Blaauw, M., Reimer, P.J., Chabangborn, A., Löwemark, L., Chawchai, S., 2012. Holocene environmental changes in northeast Thailand as reconstructed from a tropical wetland. *Global and Planetary Change* 92–93, 148–161.

Wu, X., Zhang, Z., Xu, X., Shen, J., 2012. Asian summer monsoonal variations during the Holocene revealed by Huguangyan maar lake sediment record. *Palaeogeography, Palaeoclimatology, Palaeoecology* 323–325, 13–21.

Wüst, R.A.J., Bustin, R.M., 2004. Late Pleistocene and Holocene development of the interior peat-accumulating basin of tropical Tasek Bera, Peninsular Malaysia. *Palaeogeography, Palaeoclimatology, Palaeoecology* 211, 241–270.

Yancheva, G., Nowaczyk, N.R., Mingram, J., Dulski, P., Schettler, G., Negendank, J.F.W., Liu, J., Sigman, D.M., Peterson, L.C., Haug, G.H., 2007. Influence of the intertropical convergence zone on the East Asian monsoon. *Nature* 445, 74–77.

Yang, X., Ma, N., Dong, J., Zhu, B., Xu, B., Ma, Z., Liu, J., 2010. Holocene hydrological and climatic changes in the Badain Jaran Desert, western China. *Quaternary Research* 73, 10–19.

Yang, X., Scuderi, L., 2010. Hydrological and climatic changes in deserts of China since the Late Pleistocene. *Quaternary Research* 73, 1–9.

Yang, X., Scuderi, L., Paillou, P., Liu, Z., Li, H., Ren, X., 2011. Quaternary environmental changes in the drylands of China – A critical review. *Quaternary Science Reviews* 30, 3219–3233.

Yang, X., Zhu, B., Wang, X., Li, C., Zhou, Z., Chen, J., Wang, X., Yin, J., Lu, Y., 2008. Late Quaternary environmental changes and organic carbon density in the Hunshandake Sandy Land, eastern Inner Mongolia, China. *Global and Planetary Change* 61, 70–78.

Zhang, J., Chen, F., Holmes, J.A., Li, H., Guo, X., Wang, J., Li, S., Lü, Y., Zhao, Y., Qiang, M., 2011. Holocene monsoon climate documented by oxygen and carbon isotopes from lake sediments and peat bogs in China: A review and synthesis. *Quaternary Science Reviews* 30, 1973–1987.

Zhao, Y., Yu, Z., Chen, F., Zhang, J., Yang, B., 2009. Vegetation response to Holocene climate change in monsoon-influenced region of China. *Earth-science Reviews* 97, 242–256.